

St. Petersburg State University
Institute of Earth Sciences

Khudyakova Ekaterina Nikolaevna

Master thesis

Methane fluxes and gas hydrates of the Kara and Laptev Seas shelves

Master program BM.5710.
«Cold Region Environmental landscapes Integrated Science (CORELIS)»
05.04.06 Ecology and Environmental management

Scientific supervisor: Dr. Alexey A. Krylov

Scientific consultant: Pavel Serov, postdoc

Reviewer: Dr. Pyotr B. Semenov

St. Petersburg
2020

Information about scientific supervisor, scientific consultant and reviewer

Scientific supervisor: Dr. Alexey A. Krylov, Leading Researcher, VNIIOkeangeologia, associate professor, St. Petersburg State University, Institute of Earth Sciences, Department of Sedimentary Geology

Scientific consultant: Pavel Serov, PhD, VISTA postdoc at CAGE - Centre for Arctic Gas hydrate, Environment and climate, UiT The Arctic University of Norway

Reviewer: Dr. Pyotr B. Semenov, Leading Researcher, VNIIOkeangeologia

Table of contents

Information about scientific supervisor, scientific consultant and reviver	2
Table of contents	3
Abstract in English	5
Abstract in Russian	6
1. Introduction	7
1.1. Background and importance of the research	7
1.2. Structure of the master thesis	8
1.3. The region of investigation	8
1.4. Goals and objectives	9
2. Theoretical background	10
2.1 Methane as greenhouse gas	10
2.2 Sources of methane	10
2.3 Physicochemical properties of methane	11
2.4 Impact on climate system	13
2.5 Gas hydrates origin	14
2.6 Gas hydrates distribution	16
2.7 Gas hydrates in the Arctic Region	17
3. Methodology	20
3.1 Gas hydrate stability zone	20
3.1.1 Concept of stability of gas hydrates	20
3.1.2 Hydoff (hydrate prediction program)	22
3.1.3 Bottom temperature	23
3.1.4 Bottom salinity	25
3.1.5 Geothermal gradient	28
3.2 Methane fluxes	30
3.2.1 Organic carbon content	30
3.2.2 Methane content	32
4. Results	34
4.1 Gas hydrate stability zone	34
4.2 GHSZ during late Pleistocene	48
4.3 Methane fluxes	51
5. Discussion	55
6. Conclusion	61

Acknowledgements	63
References	64
Attachment 1	68
Attachment 2	69
Attachment 3	70

Abstract

METHANE FLUXES AND GAS HYDRATES OF THE KARA AND LAPTEV SEAS SHELVES

Ekaterina N. Khudyakova

Master Program for Cold Region Environmental landscapes Integrated Science
“CORELIS” / 05.04.06 Ecology and Environmental management

Scientific supervisor: Dr. Alexey A. Krylov, VNIIOkeangeologia, Saint Petersburg State University

Scientific consultant: Pavel Serov, PhD, UiT The Arctic University of Norway

Methane is an important component of atmospheric air and a greenhouse gas, the contribution to the greenhouse effect of which is 25 times stronger than from carbon dioxide. Because the methane content in the air has been continuously growing since the pre-industrial period, this fact worries researchers around the world. If methane concentration continues to increase, the effect of global warming will be more noticeable.

Gas hydrates are one of the sources of methane that, when destabilized, can release methane into the atmosphere and thereby contribute to climate change. The Arctic region has favorable conditions for the formation of gas hydrates due to low bottom temperatures. An increase of water temperature due to global warming could lead to the release of methane from gas hydrates.

The purpose of the master thesis is to assess the potential fluxes of methane in the area of distribution of gas hydrates on the shelves of the Kara Sea and the Laptev Sea. To achieve this goal, it is necessary to determine the thickness of the gas hydrate stability zone (GHSZ) from profiles at present time and in the late Pleistocene, and calculate the amount of methane, that can be generated by microbes on the basis of the organic carbon content in bottom sediments.

For these purposes, four profiles were chosen in the Kara Sea and the Laptev Sea: 2 submeridional and 2 sublatitudinal, with 16 points located at different depths.

Calculations of the thickness of the GHSZ were made using the Hydrate software (Hydrate prediction program). Calculations of methane flows were made with help of stoichiometric method based on reaction of methane formation from organic matter.

As a result, the thickness, top and base of the GHSZ (for four gas mixtures) were calculated at all points of chosen profiles. Based on the calculations, the GHSZ thickness is lower in the Laptev Sea than in Kara Sea by an average of 200 m, which indicates its greater degree of vulnerability to methane dissociation. A 10% admixture of ethane in gas hydrates reduces the depth of potential formation of gas hydrates by an average of 100 m, and the thickness of the stability zone increases by an average of 150 m. Calculations for the late Pleistocene period showed that the thickness of GHSZ is currently greater, which is caused by an increase sea level and creating additional hydrostatic pressure.

Calculations of the amount of methane, which can be generated by bottom sediments, showed that at chosen points there is no additional deep source of methane release from gas hydrates, that means their stability at present time.

15-May-2020

Аннотация

ПОТОКИ МЕТАНА И ГАЗОВЫЕ ГИДРАТЫ ШЕЛЬФОВ КАРСКОГО МОРЯ И МОРЯ ЛАПТЕВЫХ

Худякова Екатерина Николаевна

Магистерская программа «Комплексное изучение окружающей среды полярных регионов» «КОРЕЛИС» / 05.04.06 «Экология и природопользование»

Научный руководитель: Алексей Алексеевич Крылов, к.г.-м.н., вед.н.с., ФГБУ "ВНИИОкеангеология", доцент, СПбГУ

Научный консультант: Павел Серов, кандидат естественных наук, доктор, Арктический университет Норвегии

Метан является важным компонентом атмосферного воздуха и парниковым газом, вклад в парниковый эффект которого в 25 раз сильнее, чем от углекислого газа. В связи с тем, что содержание метана в воздухе непрерывно растет с преиндустриального периода, этот факт беспокоит исследователей всего мира. Если концентрация метана продолжит возрастать, эффект глобального потепления будет все более заметен.

Газовые гидраты являются одним из источников метана, которые при дестабилизации могут высвободить метан в атмосферу и, тем самым, содействовать изменению климата. Арктический регион обладает благоприятными условиями для формирования газовых гидратов из-за низких придонных температур. Повышение температуры воды, вследствие глобального потепления, может привести к высвобождению метана из газовых гидратов.

Цель магистерской диссертации – оценить потенциальные потоки метана в районе распространения газовых гидратов на шельфах Карского моря и моря Лаптевых. Для выполнения данной цели необходимо определить мощность зоны стабильности газовых гидратов по разрезам в настоящее время и в позднем Плейстоцене, а также рассчитать количество метана, которое может быть сгенерировано микробами на основании содержания органического углерода в донных осадках.

Для данных целей были выбраны 4 разреза в Карском море и море Лаптевых: 2 субмеридиальных и 2 субширотных, с 16 точками, расположенными на разных глубинах.

Расчеты мощности зоны стабильности газовых гидратов были сделаны с помощью программы Hydoff (Hydrate prediction program). Расчеты потоков метана были осуществлены на основании стехиометрии реакции образования метана из органического вещества.

В результате во всех точках разрезов были рассчитаны толщина, кровля и подошва зоны стабильности газовых гидратов (для четырех газовых смесей). На основании расчетов, мощность GHSZ в море Лаптевых меньше в среднем на 200 м, чем в Карском море, что говорит о ее большей степени уязвимости к полной диссоциации метана. 10 % примесь этана в составе газовых гидратов уменьшает глубину потенциального образования газовых гидратов в среднем на 100 м, а толщина зоны стабильности увеличивается в среднем на 150 м. Расчеты для периода позднего Плейстоцена показали, что мощность зоны стабильности в настоящее время больше, что вызвано повышением уровня океана и созданием дополнительного гидростатического давления.

Расчёты количества метана показали, что в выбранных точках нет дополнительного глубинного источника в виде газовых гидратов, что говорит нам о их стабильности в настоящий момент времени.

15-May-2020

1. Introduction

1.1 Background and importance of the research

Methane is one of the greenhouse gases, which has an important place among the atmospheric component of the air. Methane content in the atmosphere increased intensively since pre-industrial period, and that is why this fact is under huge interest among researches. Increasing of methane content can cause change of chemical processes in atmosphere and it can change environmental situation on Earth (Science-based proposals ... 2015).

Since methane is greenhouse gas, which is 25 times more efficient than carbon dioxide, it contributes to the enhancement of the greenhouse effect. Thus, it has huge effect on global warming (Science-based proposals ... 2015).

Methane can originate from natural and anthropogenic sources. Natural sources of methane include swamps, tundra, water bodies, insects (mainly termites), methane hydrates, and geochemical processes. Anthropogenic sources are rice fields, mines, livestock, and losses in the extraction of gas and oil, biomass burning, landfills (Science-based proposals ... 2015).

Methane hydrates are one of the forms of methane storage, which in solid ice form trapped in permafrost and under the seabed. Potentially, further rising air and sea water temperature can cause to release of methane from this gas hydrates, thus accelerate the effect of global warming (Bogoyavlensky et al. 2018).

Most of gas hydrates reservoirs are located on the continental slopes of the oceans and in the Arctic Region. The necessary thermobaric conditions for the formation of gas hydrates are well expressed in arctic conditions. Low (negative) bottom water temperature are favorable for such gas hydrates formation. Increase of sea water temperature may cause release of methane from hydrates and has significant impact on climate system (Bogoyavlensky et al. 2018). That is why it is important to determine the gas hydrates stability zones in the Arctic Region to predict potential methane fluxes from the areas, where gas hydrates can be influenced by degradation because of climate change.

Gas hydrates also are indicators of the prospecting for oil and gas deposits, and many researchers were concentrated on this direction. But as we stated above it is also important to study the influence of gas hydrates on climate system.

1.2 Structure of the master thesis

This master thesis consists of six chapters.

The first chapter is introduction chapter, which determine importance and goals of the research.

The second chapter reviews background information about methane as greenhouse gas, its features, sources and impact on climate system, in particularly about gas hydrates and its distribution.

The third chapter represent methodological approach used in this master thesis, in particular it describes the concept of the gas hydrate stability zone and the program Hydoff (Hydrate prediction program), which was used to make calculations for defining of thickness, top and base of GHSZ. It also describes compounds, which are necessary for its determination: bottom temperature, bottom salinity and geothermal gradient, applied to the region of investigation. Finally, the chapter represent the method of methane amount calculation based on organic carbon content in bottom sediments.

The chapter four contains main results: calculated thickness, top and base of the gas hydrate stability zone in different points at the present time and late Pleistocene. Further, calculated methane fluxes are represented.

The chapter five contains discussion, where my results were accessed according to other works in this field of research.

Finally, in the chapter six – conclusion, I summarize key points of the research and briefly discuss main implications.

1.3 The region of investigation

The Kara and Laptev Sea shelves were chosen as region of investigation for the goals of this research.

Both seas are marginal seas of the Arctic Ocean with wide sea shelves where favorable conditions for formation of gas hydrates present.

The Laptev Sea occupies the shelf, captures the mainland slope and a small part of the ocean bed. The bottom relief of the shelf is relatively weakly crossed. Half of its total area relates to shelf depth until 50 m. In the northern part of the sea, continental slope abruptly breaks off and passes into the ocean bed, where the depths significantly increase with the maximum depth of of 3385 meters. The average depth of the Laptev Sea is 533 m (Dobrovolskiy, Zalogin 1982).

The bottom relief of the Kara Sea compared to the Laptev Sea is very uneven. Depths until 100 m predominate in the sea. The southern and eastern parts of the sea are

shallowest, the greatest depths are in the west and north-west of the Kara Sea (Dobrovolskiy, Zalogin 1982). The maximum depth is 620 m in the northern part of St. Anna Trough. Narrow Novaya Zemlya Trough stretches along Novaya Zemlya. Additionally to St. Anna Trough, Voronin Trough and the accumulative elevations including the Central Kara Rise are distinguished (Kulakov et al. 2004).

Kara Sea and Laptev Sea have more harsh climatic conditions in comparison with Barents Sea, where the influence of the Golfstream is quite significant and where we can expect increased methane fluxes because of more intensive degradation of subaquatic permafrost and gas hydrates. Nevertheless, it is important to evaluate potential methane fluxes from this region because of accelerating of global climate change in the whole Arctic Region.

1.4 Goals and objectives

The goal of the master thesis is to evaluate potential methane fluxes from gas hydrates distribution areas in the Kara and Laptev seas shelves.

Next objectives were defined:

- To determine thickness, top and base of gas hydrates stability zones (GHSZ) in different point of profiles in the Kara and Laptev Seas
- To determine thickness, top and base of GHSZ for Late Pleistocene and compare them with present time
- To calculate amount of methane which can be generated in different points of profiles on the basis of organic carbon content in bottom sediments

In this research was decided to determine where in the Kara Sea and the Laptev Sea gas hydrates can lay directly near the bottom surface. It allows us to see zones where gas hydrates more vulnerable to dissociation and where then we potentially can expect higher methane fluxes, which can contribute to further climate change.

2. Theoretical background

2.1 Methane as greenhouse gas

Methane (CH₄) has an important place among the atmospheric components of the air, which is under the huge interest among researchers. Such increased attention is explained by the fact that the methane content in the atmosphere changed significantly over the past two centuries. Since the pre-industrial period the concentration of methane increased by about 150%, while the concentration of CO₂ only 40% (Kiselev, Reshetnikov 2013). Increasing of methane content may change chemical processes in the atmosphere, which further can lead to a deterioration of the environmental situation on Earth (Science-based proposals ... 2015).

Greenhouse gases play very important role in climate system. Without greenhouse gases (CO₂, water vapor, methane and some other impurities), the average temperature on the Earth's surface would be only -23 ° C, and now it is about 15 ° C (Nauchno-obosnovannye predlozhenija ... 2015). Methane is one of the major greenhouse gases. An increase in its content in the atmosphere contributes to the enhancement of the greenhouse effect, since methane intensively absorbs the thermal radiation of the Earth in the infrared region of the spectrum at a wavelength of 7.66 microns (Science-based proposals ... 2015). The contribution of atmospheric methane to global warming is the second after the contribution of CO₂. The methane molecule is more efficient for global warming than carbon dioxide molecule: global warming potential of methane in the short term is 72, and the medium term is 25 times higher than that of carbon dioxide (Kiselev, Reshetnikov 2013).

The total amount of methane in the atmosphere is estimated around 4600-5000 Tr (Tr = 10¹² g). In the southern hemisphere, methane concentration is slightly lower than in the northern hemisphere. Such a difference can be explained by lower power of methane sources in the southern hemisphere: there is a suggestion that the main sources of methane are located on the continents, while the oceans contribute to the global methane flux not that noticeably. Methane lifetime in the atmosphere is about 8-12 years (Science-based proposals ... 2015).

2.2 Sources of methane

Most of the atmospheric methane has biogenic bacterial origin. Chemically methane is not able to form in the atmosphere. Therefore, natural methane can be only brought to the atmosphere by its flows from the earth's surface (Kiselev, Reshetnikov 2013).

Methane enters to the atmosphere from natural and anthropogenic sources, the power of latter is now higher than the power of natural (Fig. 1). The overall average annual global emission of CH₄ averages 582 Mt with a spread of 503–610 Mt. Over 1/3 of methane emissions belong to natural sources and slightly less than 2/3 to anthropogenic (Kiselev, Reshetnikov 2013).

Natural sources of methane include swamps, tundra, water bodies, insects (mainly termites), methanhydrates, and geochemical processes. Anthropogenic sources are rice fields, mines, livestock, and losses in the extraction of gas and oil, biomass burning, landfills (Science-based proposals ... 2015).

Sources of methane such as swamps, rice fields and livestock are dominant contributor to the formation of a general flow into the atmosphere. About 200 Mt CH₄ is released into the atmosphere annually due to natural sources (with a range of estimates from 101 to 355 Mt / year), the main contribution to which are swamps. 50% of swamp area are located in the countries of the Arctic region, and thus share of these countries in the methane emission is estimated at 30-50% (Kiselev, Reshetnikov 2013).

The heterogeneity of methane sources is the main reason for the large errors in the estimates of their intensity (Kiselev, Reshetnikov 2013).

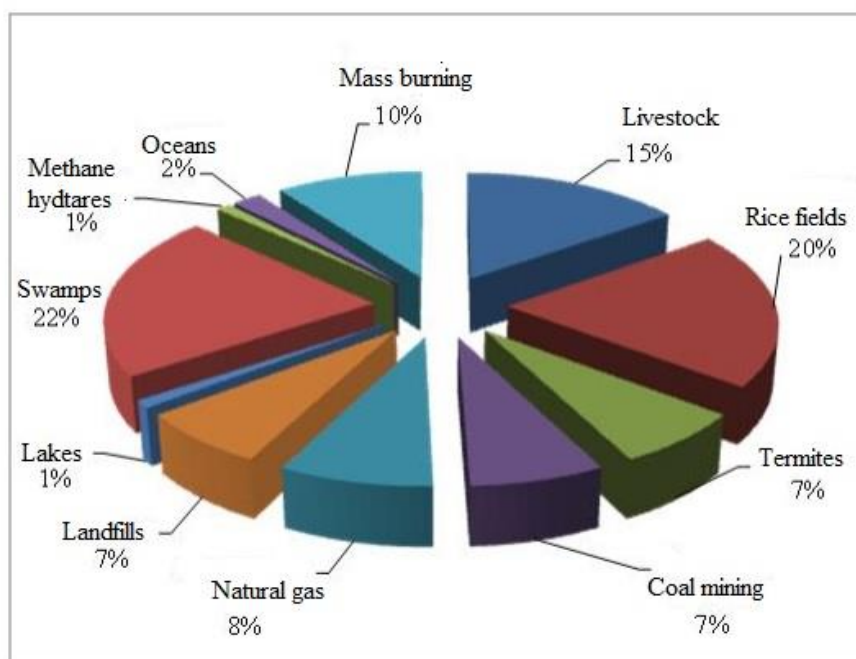


Figure 1. Methane sources (Science-based proposals ... 2015).

2.3 Physicochemical properties of methane

Methane is colorless, non-toxic, odorless and tasteless gas. Methane contains 75% carbon and 25% hydrogen. 1 nm³ (normal cubic meter - the reduced volume of gas

to the volume of 1 m³ of liquid) has a mass of 0.717 kg. Slightly soluble in water, lighter than air. Methane is non-toxic and non-hazardous to human health. Accumulating indoors, methane is explosive (Science-based proposals ... 2015).

Methane is the most important representative of organic matter in the atmosphere. The main component of natural (77-99%), associated petroleum (31-90%), mine and swamp gases. Under anaerobic conditions (in swamps, wetlands, the rumen of ruminants) methane is formed biogenically. It also turns out during coking of coal, hydrogenation of coal, hydrogenolysis of hydrocarbons in catalytic reforming reactions (Science-based proposals ... 2015).

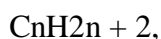
Methane molecule has a tetrahedral structure with sp³-hybridization of the carbon atom (Figure 2).



Fig. 2 Methane molecule (Physical and chemical properties of natural gas 2008)

Methane has a relatively low reaction ability. This is because the rupture of the four bonds in methane molecule requires a large expenditure of energy.

Methane is the simplest representative of the class of alkanes, forming a homologous series. Methane hydrocarbons are called homologues, having the general formula:



where n is a carbon number equal to 1 (for methane), 2 (for ethane), 3 (for propane), etc.

Each subsequent homologue differs from the previous one by one -CH₂ group (Physical and chemical properties of natural gas 2008).

Methane determines the physicochemical properties of the homologous series of alkanes. Under normal conditions, methane and its homologs are inactive and react under the action of high temperature and catalyst. Additional conditions are necessary for splitting the C – H bond. With the increase in the number of atoms in the molecule

of heavy hydrocarbons their density and heat of combustion increases (Physical and chemical properties of natural gas 2008).

Basic physical properties of methane (Physical and chemical properties of natural gas 2008):

- lighter than air;
- odorless and tasteless;
- poorly soluble in water;
- molecular weight – 16 g/mol;
- melting point is – -182.49 ° C;
- boiling point – -161.56 ° C;
- flash point - 87.8 ° C;
- autoignition temperature - 537.8 ° C.
- methane density – 716 kg/m³ or 0.716g/cm³

2.4 Impact on climate system

Climate change in the Arctic Region may have significant influence over global climate. Emission of greenhouse gases, together with surface reflectivity and ocean circulation are major mechanisms or feedbacks that affect global climate change.

Most of carbon is currently stored in the form of organic matter trapped in permafrost area. Most of this organic matter are concentrated in wetlands of Siberia and North America. Decomposition and releasing of methane and carbon dioxide occurs during the summer, when upper layer of permafrost is thawing. Further warming may increase and accelerate this carbon release and amplify feedback in additional release, causing more warming and so on (ACIA 2004).

Another source of carbon in the form of plant material are stored in boreal forests and arctic tundra. Decomposition of dead plant material in mires and tundra ponds leads to producing of methane. Rising temperature and precipitation generally accelerate release of methane and carbon dioxide to the atmosphere (ACIA 2004). As it was said before, methane is 25 times stronger greenhouse gas then carbon dioxide.

Another form of methane storage are methane hydrates, which in solid ice form trapped in permafrost and under the seabed. Consequently, thawing of permafrost and rising of water temperature can lead to methane release from this gas hydrates. If such release may potentially happen, impacts for climate could be huge (ACIA 2004).

2.5 Gas hydrates origin

Natural gas hydrates are termed “clathrates” or inclusion compound (Koh et al. 2010). Hydrates, are a specific combination of water and natural gas. If these compounds meet under specific conditions with high pressure and low temperature, they join to form a solid, ice-like substance (Collett et al. 2000).

The basic hydrate unit consists of a hollow crystal of water molecules with a one molecule of gas floating inside. The crystals coalesce in a tight latticework. Hydrates are also called gas hydrates, methane hydrates, or clathrates. Clathrates are formed from the Greek and Latin words “cagework”. Hydrates look like ice, but they have gas molecules, which presented within crystals. Hydrates are similar to ice, but they are able to burn when set fire with a match (Collett et al. 2000).

In a gas hydrate crystal, a water molecule forms a framework (host lattice) in which there are cavities. The frame cavities are usually 12-facets ("small" cavities, which corresponds to D and D'), 14-, 15-, 16- and 20-facets ("large" cavities, which corresponds to T, T', P, H и E). General view of small (D and D') and large cavities (T, T', P, H и E) are shown on the figure 3. Oxygen atoms are tops, and hydrogen bonds are ribs. These cavities can be completely or partially occupied by gas molecules (“guest molecules”). The gas molecules are connected to the water frame by van der Waals bonds (Reshetnikov, Golovanchikov 2010).

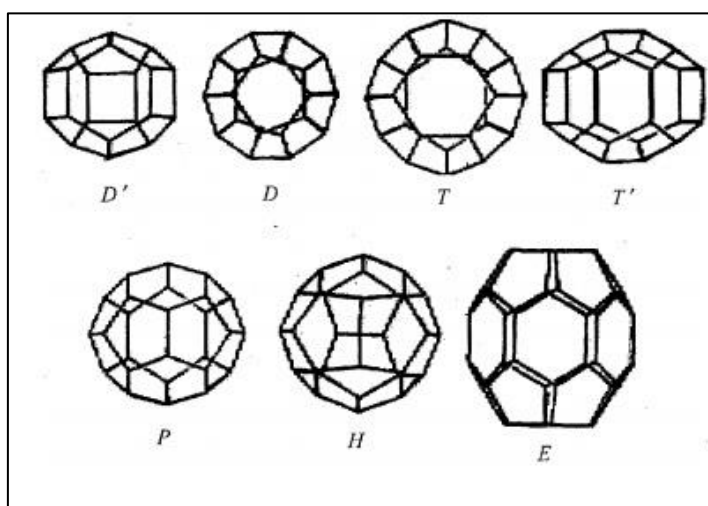


Fig. 3 General view of small (D and D') and large cavities (T, T', P, H и E) (Reshetnikov, Golovanchikov 2010)

Cavities, combining with each other, form a continuous structure of various types. According to the accepted classification, they are called KS, TS, HS - cubic, tetragonal and hexagonal structures, respectively. In nature, hydrates of the KCI, KS-II

types are most often found, while the rest are metastable (Reshetnikov, Golovanchikov 2010).

The crystal structure of gas hydrates depends on the size of the guest gas molecules. For example, KS-I hydrates form gases with a molecular size of 0.43-0.58 nm. The structure of KS-I is formed by individual gases, such as methane, ethane, carbon dioxide. KS-II hydrates are formed if the size of the guest molecule is 0.58-0.72 nm. The KS-II structure is formed by gases: oxygen, nitrogen, propane, argon (Drachuk 2018).

According to Sloan (2008) two hydrate crystal structures (sI and sII) were determined in the late 1940s and early 1950s by von Stackelberg and coworkers. The third hydrate structure, structure H (sH) was discovered only in 1987. Hydrate crystal unit structures sI, sII and sH are shown on the Fig. 4.

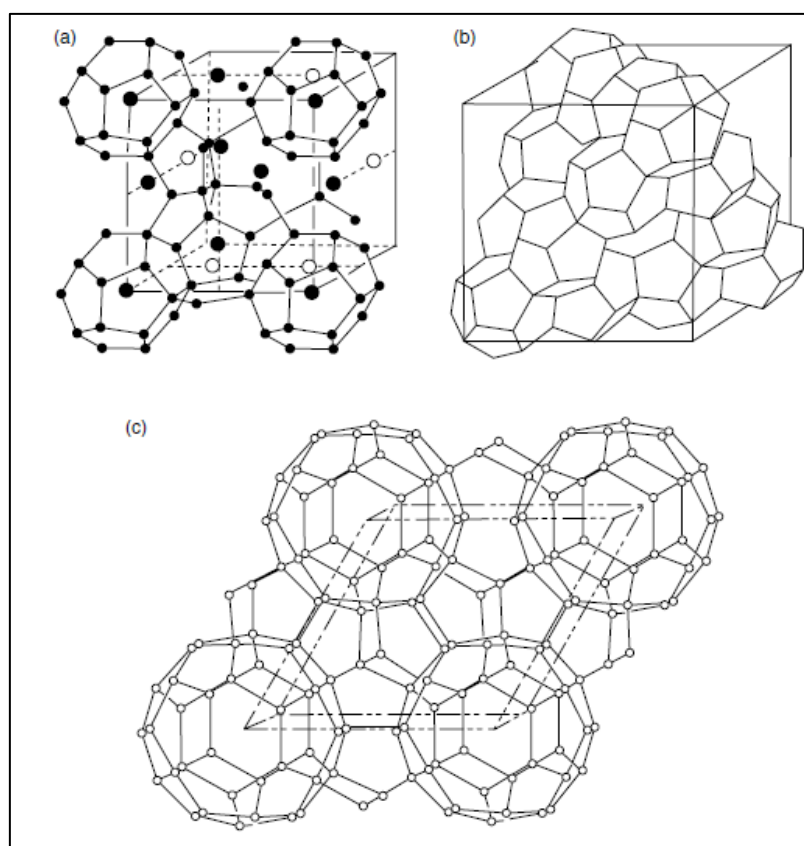


Fig.4. Hydrate crystal unit structures: (a) sI, (b) sII, and (c) sH. (Sloan 2008)

While sI, sII, and sH are the most common clathrate hydrates, a few other clathrate hydrate phases have been identified. These other clathrate hydrates include new phases found at very high pressure conditions (i.e., at pressures of around 1 GPa and higher at ambient temperature conditions) (Sloan 2008).

Hydrates are known among chemists for almost 200 years, but until recently, these matter were treated as laboratory curiosities. The oil industry started to be

interested in hydrates in the 1930s when gas-hydrate caused problems with pipeline blockage in Kazakhstan. Since that time, hydrates were studied in the direction of escaping and prevention of their accumulation in pipelines and oil industrial structures (Collett et al. 2000).

In the 1960s, naturally occurring hydrates were discovered by a Russian drilling crew in a Siberian gas field. Then, in the 1970s, naturally occurring hydrates were detected not only in polar continental regions but also in sediments on the peripheral areas of the ocean (Collett et al. 2000).

Many researchers suggest that the gas that is presented in naturally occurring hydrates is generated by anaerobic bacteria, which destroy organic matter under the seafloor and then produce methane and other gaseous products such as carbon dioxide, hydrogen sulfide, ethane and propane. All of these gases can be incorporated in gas hydrates, but methane predominates. In a limited number of settings, methane in gas hydrates also can be thermogenic origin, which comes from sources deeper within the earth (Collett et al. 2000).

Methane is packed effectively in a compact gas hydrate structure. A cubic volume of hydrate contains gas that will expand to somewhere between 150 and 180 cubic volumes at standard pressure and temperature (Collett et al. 2000).

2.6 Gas hydrates distribution

Vast volumes of sediments in the ocean bottoms and polar regions are suitable to formation of gas hydrates (Collett et al. 2000). The zone of stability of gas hydrates in the waters of the world ocean confined to areas with a depth of sea a bottom from 200 m for subpolar regions and from 500 - 700 m for equatorial conditions (Богоявленский и др. 2018). In polar regions, gas hydrates can be formed at shallower depths because the lower surface temperatures (Collett et al. 2000). Organic matter in water areas accumulates mainly in peripheral areas of the ocean, including shelves and continental slopes. Significantly less organic matter is deposited on abyssal plains of deep ocean zones. In this connection, the most favorable conditions for the formation of gas hydrates are the areas of the deep-water shelf and the continental slope. By modern estimates, 98% of all gas hydrates are concentrated in the waters of the oceans, while on land only 2% (Bogoyavlensky et al. 2018). Gas hydrates are potentially natural seafloor carbon sink and they are involved in the global carbon cycle. Methane, ethane, propane and other gases are stored in gas hydrates and can be released over time (Serov et al. 2017).

Gas hydrates deposits have been detected in Japan, in the US eastern seaboard in the Blake Ridge, near the continental margin of Vancouver, British Columbia, Canada, and offshore New Zealand. Gas hydrates which were identified by direct sampling are insignificant. Most of accumulations are predicted by indirect sources, such as seismic reflections, well logs, drilling data and pore-water-salinity measurements (Collett et al. 2000).

So, the largest part of open reservoirs of has hydrates is located on the continental slopes of the oceans and in the Arctic, as seen on the map on figure 5.



Fig. 5. Distribution of gas hydrates in the Arctic and the World Ocean. 1 — proved by direct research including drilling; 2 — well logging forecast; 3 — indirect signs, including seismic data (BSR). (Bogoyavlensky et al. 2018).

2.7 Gas hydrates in the Arctic Region

Thermobaric conditions for the formation of gas hydrates exist in the majority of the water area of the Arctic Ocean and almost throughout the Russian Arctic shelf, including the region Shtokman gas condensate field in the Barents Sea, where negative water temperature was measured at a depth of more than 300 m (about -1.5°C). This fact is significant complicated the development of this field, as there were additional problems associated with the possible formation of man-made gas hydrates in wells and subsea pipelines (Bogoyavlensky et al. 2018).

Due to the huge area of the Russian shelf Arctic and the almost ubiquitous existence of the permafrost region, it is reasonably assumed that the largest resources of gas hydrates are concentrated here. However, gas hydrates has not yet been identified

on any of areas of the Russian Arctic, and on adjacent land they are only predicted in varying degrees of probability in a few places, including proven core existence of wells of the Bovanenkovskoye and Yamburgskoye fields. On the famous Messoyakha field the presence of gas hydrates is predicted, but no direct evidence has yet been obtained. This does not confirm the rarity of gas hydrates, but testifies to the deficiencies of the search works. Traditional oriented drilling technology on deep sediments do not imply studies of the presence of gas hydrates. At the same time, as a result of targeted research within other water areas of Russia gas hydrates were found in many areas of Okhotsk, Caspian and Black seas, as well as at the bottom of Lake Baikal (Bogoyavlensky et al. 2018).

Cartographic scheme of gas hydrates distribution in the Circumpolar region is shown on Fig. 6.

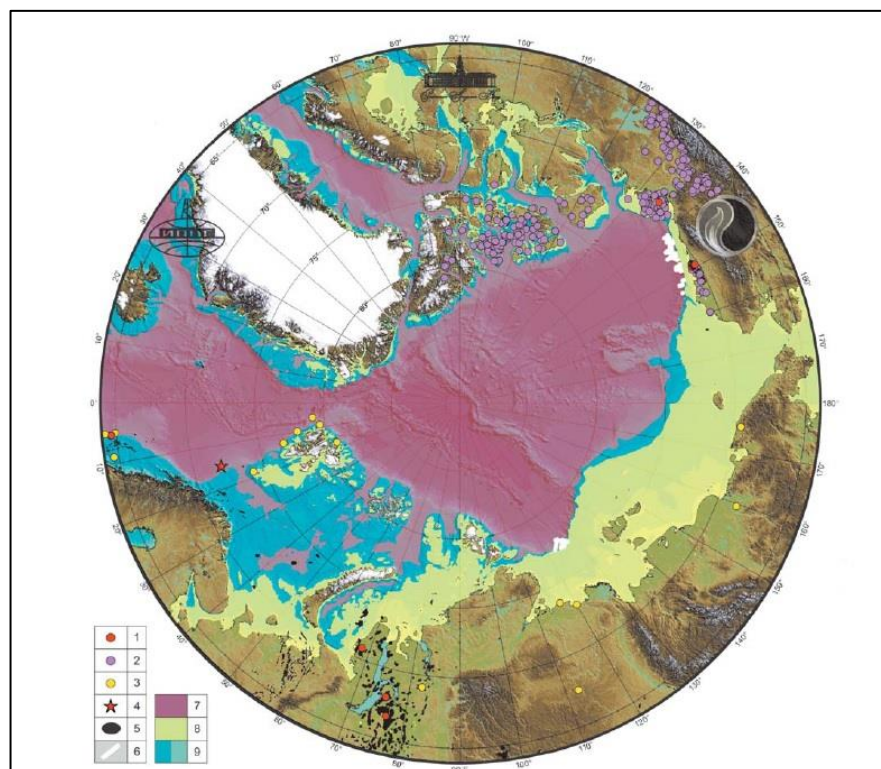


Figure 6. The scheme of distribution of gas hydrates in the Circumpolar Region (cartographic basis of IBCAO). Legend: 1— gas hydrates confirmed by samples from the bottom of the well, 2 — highly probable well logging forecast wells, 3 — BSR and other indirect signs of gas hydrates, 4— mud volcano Haakon Mosby with gas hydrates, 5 — traditional oil fields and gas, 6 □ — BSR zones in the seas of Laptev and Beaufort, 7— zone of favorable thermobaric conditions, 8 — favorable zone of subaqual permafrost, 9 □- lack of conditions for the formation and existence of gas hydrates in the waters (Bogoyavlensky et al. 2018).

In addition to the zone of favorable thermobaric conditions for modern formation and the preservation of gas hydrates on the Arctic shelf, there is an area of the

proposed development of subaqueal permafrost, which is a zone of gas hydrates metastability in which due to the effect of self-preservation, relict gas hydrates can be preserved. The last glacial maximum occurred at the end of the late Pleistocene (25–19 thousand years ago). At this time, the level of the World Ocean dropped significantly (according to various sources to 105-163 m), since large water volumes left the hydrosphere of the World Ocean and went into a frozen state in ice sheets up to 3-4 km thick. Vast areas of the modern shelf of the Arctic Ocean have become dry land and in the low-lying parts powerful (sometimes more than 1 km, as in Yakutia) zones of permafrost and associated gas hydrates. After the end of the ice age (about 9 thousand years ago) and climate warming in the last millennia, the glaciation retreated, and the level of the World Ocean rose by about 120 m. At the same time, the process of gradual degradation of subaqueal permafrost began. One of the reasons that permafrost have not completely degraded so far is the low (negative) bottom water temperature. This means that at the present time we can predict the spread of relict metastable gas hydrates on the shelf to a depth of 120 m (Bogoyavlensky et al. 2018).

3. Methodology

3.1 Gas hydrate stability zone

3.1.1 Concept of stability of gas hydrates

From the very beginning of research on gas hydrates, it was found that the hydrates of various individual gases are formed in a strict range of pressures and temperatures, and each gas has its own specific range. Some gases (mainly artificially synthesized) form hydrates at atmospheric pressure and temperatures around 0 ° C, but for natural gases, hydrate formation conditions are characterized by higher pressures and lower temperatures (Yakushev 2009).

The most common gas in the permafrost area is methane. However, pure methane can be met extremely rare. Impurities of other gases in a small amount (such as nitrogen, carbon dioxide, hydrocarbon homologues of methane, hydrogen sulfide) are present in the composition of the main gas practically always and they may change the conditions of hydrate formation (Yakushev 2009).

Of particular importance is the effect on the phase equilibrium of gas hydrates with water-soluble salts, which are almost always present in the pores of the dispersed rocks of the cryolithozone.

If we match the curve of thermodynamic conditions of hydration to real curves of the distribution of temperatures and pressures over the depth of the earth's crust, we can get their intersection in a number of geographic areas of the Earth. This is because in most regions the distribution of temperatures and pressures in depth has a character close to linear, and the hydration curve in linear coordinates is a parabola. And where the crust is exposed to cooling and / or high pressures, there are favorable conditions for the formation of hydrates (Yakushev 2009).

Thus, when comparing the thermodynamic conditions of hydrate formation (taking into account the composition of the gas, the mineralization of pore waters and the influence of the mineral matrix) and the thermodynamic and geochemical conditions existing in the rocks, it is possible to identify an area favorable for hydrate formation - gas hydrates stability zone (Yakushev 2009).

Gas hydrates stability zone is the part of the lithosphere and hydrosphere of the Earth, the thermodynamic and geochemical regimes of which correspond to the conditions for the stable existence of gas hydrates of a certain composition (Yakushev 2009).

Gas hydrates are stable only under specific conditions where pressure is high and temperature is low. The space where gas hydrates are stable is called the gas hydrate stability zone (GHSZ). It is determined by the intersection of the pressure-temperature phase boundary and the local geothermal gradient. Because of specific conditions for stability, gas hydrates are usually can be formed only in polar regions and on continental slopes where water depth exceeds 300–500 m (Amundsen, Landro 2012). According to Serov et al. (2017) GHSZ is a function of bottom water temperature, hydrostatic and lithostatic pressure, meaning of geothermal gradient, water salinity, and the composition of the gases in gas hydrates. Generally, than greater water depth than more thickness of GHSZ.

As shown in the figure 7 (b) for the marine setting, the top of the GHSZ occurs above the sea floor. However, the ocean water does not contain enough gas to stabilise hydrate and the top of the GHSZ is normally defined at the sea floor. Here, the temperature is normally 3–4°C. Going down into the sediment, the temperature slowly increases; the global average of the geothermal gradient is 0.02°C/m. While the pressure increases with depth, after 500–1,000 m depth the temperature becomes too high for hydrates to remain stable. This is the base of the GHSZ (Amundsen, Landro 2012).

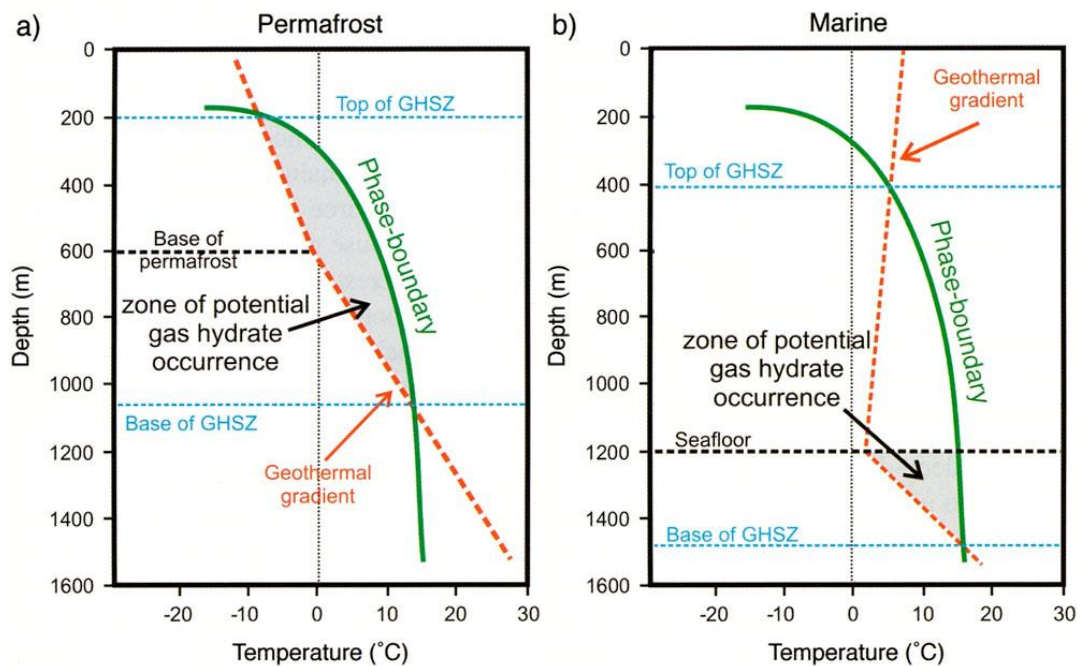


Figure 7. GHSZ for a) permafrost and b) marine cases (Amundsen, Landro 2012).

In permafrost (a), the situation is similar. The top of the GHSZ is where the temperature line crosses the hydrate stability line, often beginning at 100–300 m depth. The GHSZ typically extends for hundreds of meters. The depth of the GHSZ is also

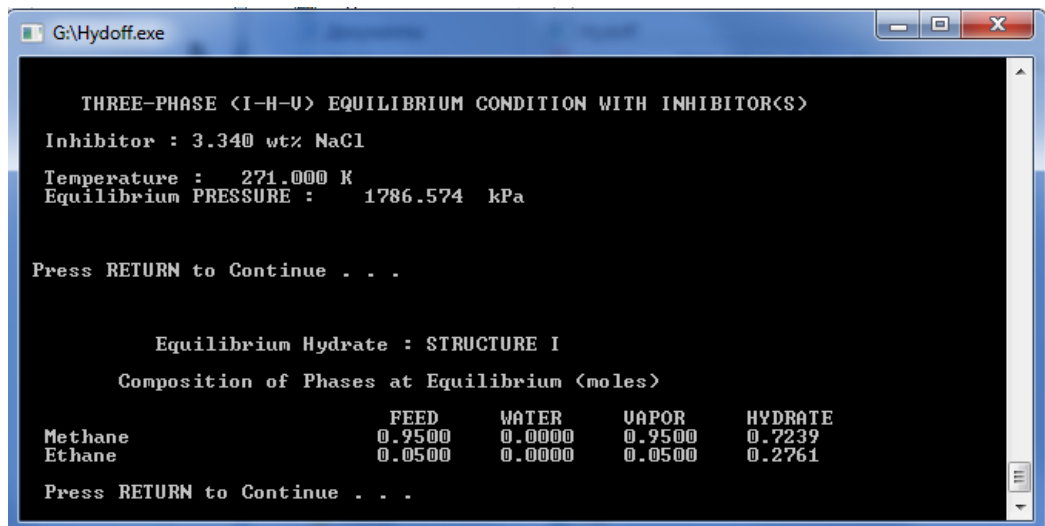
related to the base of the permafrost, which is at 0°C. The deeper the base of the permafrost the deeper the GHSZ becomes (Amundsen, Landro 2012).

3.1.2 Hydooff (Hydrate prediction program)

To calculate the stability of gas hydrates, the program Hydooff (Hydrate prediction program) was used. The description of the Hydrate prediction program is represented in monograph by E. Sloan (1998).

The program is able to provide the information about hydrate phase equilibria with and without thermodynamic inhibitors. The program can show pressure predictions of gas hydrates of structure I and II at a given temperature with and without thermodynamic inhibitors (methanol, salt (NaCl), or mixtures thereof) at three- and four-phase conditions (I-H-V, LW-H-V, LW-H-V-LHC) (Sloan 1998).

The interface of the program Hydooff is shown on the figure 8.



```
G:\Hydooff.exe
THREE-PHASE <I-H-V> EQUILIBRIUM CONDITION WITH INHIBITOR(S)
Inhibitor : 3.340 wt% NaCl
Temperature : 271.000 K
Equilibrium PRESSURE : 1786.574 kPa

Press RETURN to Continue . . .

Equilibrium Hydrate : STRUCTURE I
Composition of Phases at Equilibrium <moles>
Methane      FEED    WATER   UAPOR   HYDRATE
Ethane       0.9500  0.0000  0.9500  0.7239
              0.0500  0.0000  0.0500  0.2761

Press RETURN to Continue . . .
```

Figure 8. Interface of the program Hydooff

Before the calculation in the program, the user should enter some basic information, for example: units that the user will operate in, components present in the feed, feed composition, temperature, type and amount of thermodynamic inhibitor(s) and so on. The menu of the Hydooff directs the user to the desired type of calculation. When the user choose particular calculation, the program requires to enter the temperature, and if necessary, concentration of thermodynamic inhibitor(s) in the free aqueous phase (Sloan 1998).

The standard output for hydrate phase equilibria calculations will display next results in depending from type of calculation (Sloan 1998):

1. Equilibrium phases (I-H-V, LW-H-V or LW-H-V-LHC).
2. Equilibrium pressure.

3. Hydrate equilibrium crystal structure (sI or sII).
4. Phase components and compositions (i.e. feed, fluid hydrocarbon, and hydrate).
5. Fractional occupancy of cages by hydrate formers in each type of hydrate cavity.

In the case of this research equilibrium pressure will be defined. After that it will be transformed to the depth where gas hydrate with entered characteristics may exist on the basis of unit conversion of $1 \text{ kPa} = 0.10197162 \text{ meters}$.

To get equilibrium pressure next input characteristics should be taken in account: bottom temperature, bottom salinity and gas composition.

Meaning of geothermal gradient is necessary to define the base of GHSZ.

Further, these characteristics will be discussed applicable to research region.

3.1.3 Bottom temperature

The bottom temperature, by which we understand the temperature of rocks at a certain depth from its surface, where the amplitude of annual fluctuations does not exceed $0.1 \text{ }^{\circ}\text{C}$, is one of the most important characteristics when analyzing the thermobaric conditions of the geological section within the water area. It is determined by the temperature of the bottom water, the patterns of formation and distribution of which can be established according to direct observations (Soloviev et al. 1987).

On a large area of the Arctic shelf seas, the bottom water temperature varies both during the year and over a number of years with an amplitude of $2 \text{ to } 14 \text{ }^{\circ}\text{C}$. Subaqueal conditions limit a set of factors affecting the bottom temperature to almost one — the average annual temperature at the bottom sediment-water interface.

The Arctic shelf, with the exception of a large part of the Barents Sea, the northwestern part of the Kara Sea, the deepwater straits and bays of the Canadian Arctic Archipelago and the Bering Strait, even in summertime is characterized by a significant distribution of negative-temperature bottom water. Under the influence of solar radiation, only the surface layer of the water column warms up (Soloviev et al. 1987).

In the mouth areas of the seas, the temperature of the bottom waters is determined by the magnitude of the thermal runoff of the rivers. The main heat falls in June-July. During this period, the temperature of the bottom waters reaches $4 - 6 \text{ }^{\circ}\text{C}$, but quickly drops towards the open sea to negative values. Positive bottom water temperature is observed for 2 - 3 months only in shallow waters. In winter, the entire thickness of the shelf waters has a low negative temperature, equal to the freezing point

of water at a given salinity. The amplitude of annual fluctuations in bottom water temperature in open areas of the sea varies from 0.5 to 2 °C, in shallow waters it increases to 4-8 °C, and in the mouths of large rivers it reaches 12-14 °C (Soloviev et al. 1987).

Thus, the main area of the bottom of the Arctic seas within the shelf is characterized by a negative (-1.5 degrees and below) average annual temperature. The positive average annual temperature values are confined to the mouths of the rivers, as well as to the routes of the movement of the Atlantic and Pacific waters (Soloviev et al. 1987).

Bottom temperature of Kara and Laptev seas are represented at the map on figure 9 which was cut from the entire map of bottom temperature of Arctic Ocean in Soloviev et al. 1987.

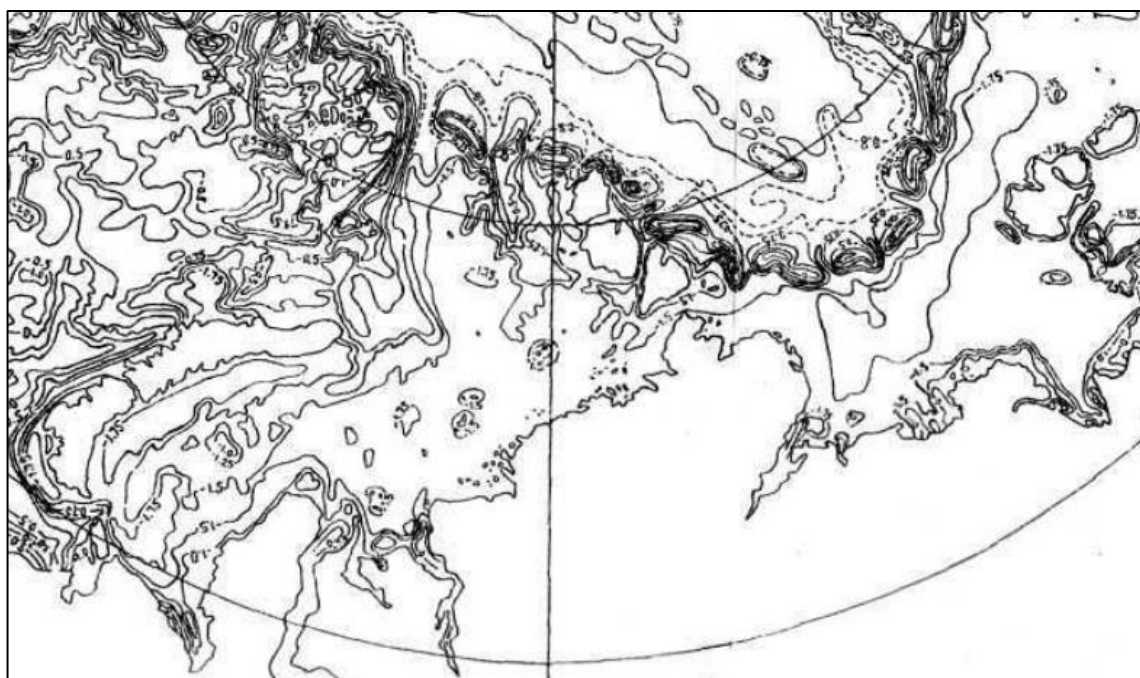


Fig. 9. Bottom temperature of the Kara and Laptev seas (Soloviev et al. 1987)

Almost the entire Kara Sea basin is filled with arctic waters. In accordance with this, the bottom temperature is characterized by low negative values (-1 to -1,87 °C). The coldest areas with a bottom temperature of -1.75 ° and below are the Novaya Zemlya Trough and the Ugorskaya basin. In the St. Anne's Trough and the Voronin Trough, when mixing negative-temperature shallow waters with positive-temperature Atlantic waters, bottom waters from -0.1 to -1.6 °C form. Transformed waters enter the deep-water part of the basin, forming a negative-temperature regime of the bottom along the route of their movement (Soloviev et al. 1987).

The temperature regime of the Laptev sea bottom is characterized by a poorly differentiated stable low (from -1.0 to -1.75 °C and below) negative temperatures. The areas of positive bottom temperatures are confined to the estuaries of rivers Lena, Yana, Olenek and others (Soloviev et al. 1987).

3.1.4 Bottom salinity

Kara Sea

In the distribution of the bottom salinity of the Kara Sea, the Baydaratskaya Bay and areas adjacent to the Yamal Peninsula are distinguished. Its lowest values are observed: 28.83–34.42 ‰ in the Baydaratskaya Bay, 29.91–33 ‰ near the Cape Kharasavey and 29.36–33 ‰ near the Bely Island. The division of the Baydaratskaya Bay into less salty south-south-west and more salty north is explained by the significant freshening of the first due to the ice melting and river runoff and the influence of the more saline Barents Sea waters dominating in the adjacent part of the sea. The low salinity values to the west of Cape Harasavey can be explained by the river runoff in this region: the Se-Yaha, Nadu, Kharasavei, Tiutei and other smaller rivers (Ermakova, Novikhin 2011).

The strongly freshened area near the Bely Island and to the north of it is area with lower values of salinity (in the area to the north of the Ob and Gydan Bays and Yenisei Gulf salinity is 31.80–33.02 ‰, and to the north-west of the Taimyr Peninsula - 33–33.39 ‰). All this water area belongs to the zone of direct influence of river flow. Negative temperatures indicate the winter origin of the bottom water masses in the area, and convective mixing (mainly due to ice formation) serves as a mechanism for the spread of low salinity values to the bottom horizons (Ermakova, Novikhin 2011).

The maximum salinity with 34.79–34.95 ‰ is observed in St. Anne's trough and in the central part of the Novaya Zemlya trough in the deepest water area up to 399 m (34.6–34.7 ‰). In the first case it is explained by the influx of waters of Atlantic origin, and in the second, influence on the formation of local water masses by the Barents Sea waters flowing with the East Novaya Zemlya current.

The deep Barents Sea waters flowing through the straits of the Kara Gates and the Yugorskiy Shar have a great influence on the rather deep-water south-western part of the sea: the salinity values on the bottom horizons here 34–34.65 ‰. Almost the same (34–34.59 ‰) values are observed near the south-western coast of the Severnaya Zemlya archipelago with depth up to 180 m (near south of the island of the October

Revolution). Apparently, this is caused by the lack of the river flow influence on this area and because of its depth. The rest of the bottom water masses in the Kara Sea have salinity is 34–34.4 ‰, which is due to their winter origin and indirect effect of the Barents Sea and Atlantic waters (Ermakova, Novikhin 2011). Bottom salinity of the Kara Sea according to Ermakova and Novikhin (2011) is shown on the figure 10.

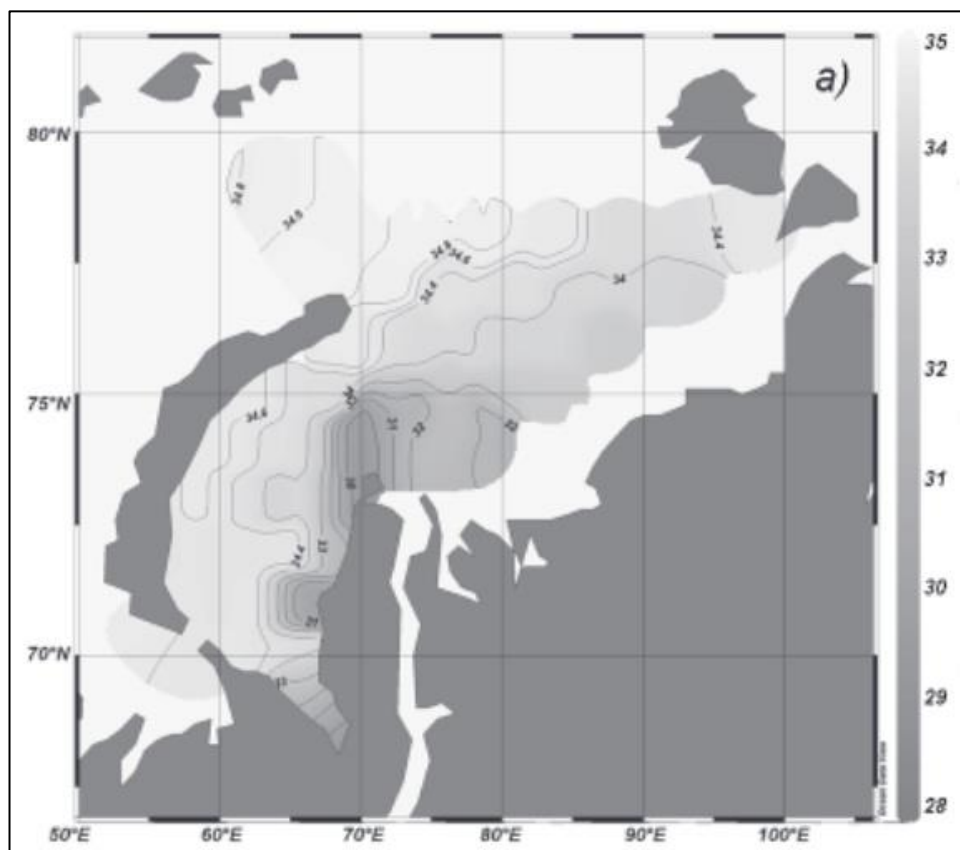


Figure 10. Bottom salinity of Kara Sea in 2007 (Ermakova, Novikhin 2011).

Laptev Sea

Salinity in the Laptev Sea is very heterogeneous: in summer it varies from 1 to almost 31 ‰, but desalinated water with a salinity of 20-30 ‰ prevails in the surface layer, and its distribution is very difficult. In general, it increases from southeast to northwest and north (Bauch et al. 2010).

Salinity increases with depth, but there are seasonal differences in its distribution. In winter, in shallow water, salinity rises from surface to horizons of 10-15 m, and further till the bottom it is almost unchanged. At great depths, salinity increases from the underlying horizons. The spring salinity distribution begins from the time of intensive snow and ice melting. Thus, values of salinity decrease in the surface layer rapidly, while at lower horizons winter values are saved (Bauch et al. 2010).

In summer, in the areas of river water influence, the upper layer (5-10 m) is strongly desalinated, with an abrupt rise in salinity below. In a layer from 10 to 25 m,

the salinity gradient in some places can be 20 ‰ per 1 m. In the northern part of the Laptev sea, salinity increases relatively quickly from the sea surface to 50 m depth, hence salinity increases more slowly to 300 m from 29 to 33 - 34 ‰, deeper it is almost unchanged (Bauch et al. 2010).

On the fig. 11 and 12 we can see maps of salinity distribution on depth 30 m and 100 m respectively (maps are taken from official web-site FSBI “Arctic and Antarctic Research Institute”). With rising depth we can observe increasing in salinity meanings.

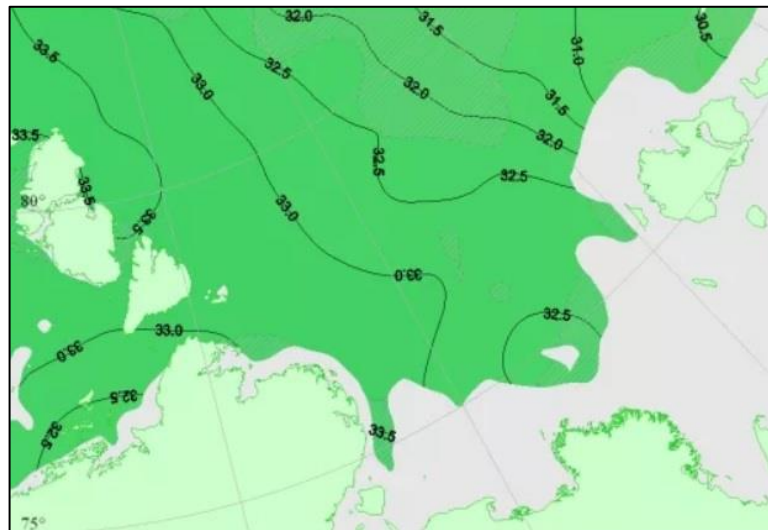


Fig.11 Laptev Sea salinity on the depth 30 m

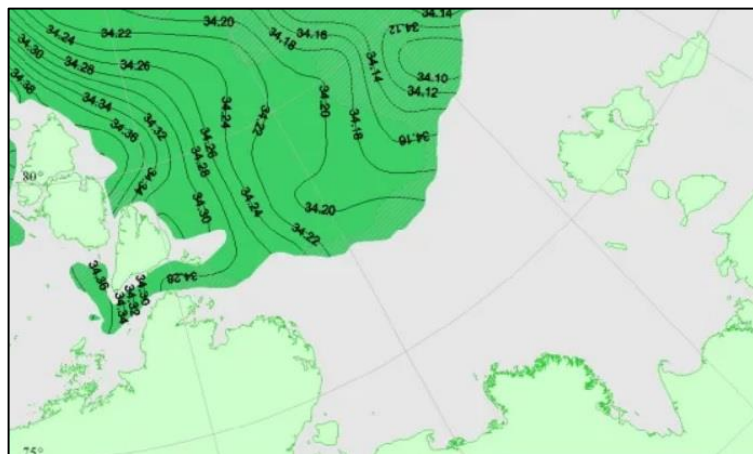


Fig.12 Laptev Sea salinity on the depth 100 m

On the figure 13 we can see salinity distribution from 73 to 77° N in 2007. According to this profile bottom salinity change from about 30 ‰ in the southern part of the shelf to about 33,8 ‰ in northern and deeper part of the shelf.

In the deeper horizons of the northern part of the Laptev Sea, from 800–1000 m and to the bottom, cold bottom water with almost uniform salinity prevails (34.90–34.95 ‰).

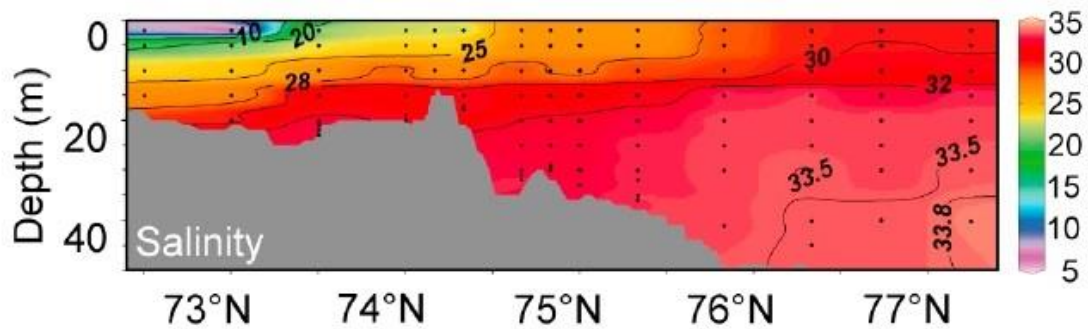


Figure 13. Salinity distribution on a south-to-north oriented section in Laptev sea in 2007 (Bauch et al. 2010)

3.1.4 Geothermal gradient

Geothermal gradient is a physical characteristic that describes the increase in the temperature of rocks in °C on a certain part of the earth. Mathematically expressed as a change in temperature per unit depth. In geology, when calculating a geothermal gradient, 100 meters are taken per unit depth. Typically, the geothermal gradient ranges from 0.5-1 to 20 °C and averages around 3 °C per 100 meters (GUFO.ME).

In different areas and at different depths, the geothermal gradient is not constant and is determined by the composition of the rocks, their physical state and thermal conductivity, the density of heat flow, proximity to intrusions and other factors. The geothermal gradient can vary quite significantly, not only in different areas, but also within the same area. (GUFO.ME).

Various tectonic elements, differing in the history of geological development, are characterized by considerable heterogeneity of the distribution of heat fluxes, which depend primarily on the depth, age and degree of fragmentation of the basement. It has been established that the intensity of heat flux increases over large positive structures and zones of deep faults. Minimal heat fluxes are observed on the platforms and especially on the Precambrian shields, in deep-sea basins, maximum - on mid-ocean ridges, rift zones and areas of modern volcanism. The heat flux increases in the direction from the ancient to the young areas of folding, and in each of them an increase in the fluxes from the foothill troughs to the areas of active orogenesis are observed. In tectonically active areas, there is a sharp differentiation of heat fluxes, for example, a tripling from marginal deflection to areas of Cenozoic folding. For oceanic plates, a regular decrease in the average values of the heat flux is observed with increasing distance from the mid-ocean ridges and, accordingly, with increasing age of the oceanic lithosphere (Khmelevskoy et al. 2004).

Marine geothermal studies are associated mainly with the upper layer of sediments, the thermal state of which consists of two components: deep and exogenous. Significant effect on geothermal regime of marine sediments can be caused by insolation and further fluctuations of bottom temperature. This is mostly typical for shelf areas of Arctic Ocean. The thermohaline state of the water column is one of the leading climate-forming factors of the Arctic marine system, and the Arctic Ocean and the adjacent waters of the North Atlantic occupy a very special position in the system of global ocean circulation (Khutorskoy et al. 2013).

Offshore seas of Arctic Ocean with relatively shallow bottom associated with the influence of exogenous periodic temperature fluctuations at the bottom – water boundary, due to seasonal and annual climate fluctuations. With a bottom depth of less than 300 m, measurements are taken inside the solar thermal zone, i.e. in the geosphere, where the effect of insolation affects. The lower boundary of the heliothermozone is the "neutral layer" - below it the temperature distribution can be considered quasistationary, depending only on the distribution of internal sources and heat sinks (Khutorskoy 2013). Below the neutral layer, the temperature of the rocks increases on average by 3.3 ° C when immersed for every 100 m. It is established that the main source of heat on the continents is the energy of radioactive decay. This is due to a higher concentration of radioactive elements in the crust than in the mantle. In the oceans, where the thickness of the Earth's crust is small, the main source of heat are the processes in the mantle at depths of 700–1000 km (Khmelevskoy et al. 2004).

The shelf of the Kara Sea is part of the eastern part of the West Arctic metaplatform. In the structure of the sedimentary cover can be traced its connection with the West Siberian plate. The platform sedimentary cover is composed mainly of the terrigenous rocks of the Phanerozoic, whose thickness varies from 1.6 (Sverdrup Island) to 14 km (South Kara Basin).

Relatively increased heat fluxes (more 70 mW / m²) are observed on the west coast of Yamal and in the South Kara basin. These points are confined to gas and gas condensate fields: the Kharasaveysky, Bovanenkovsky and Kruzenshternovsky fields on the west coast of Yamal, as well as the Leningrad and Rusanovsky fields on the Kara shelf. The connection between the localization of hydrocarbon deposits and increased heat fluxes is obvious. Lower heat flux is characteristic of the Yamalo-Gydansk syncline (Bely Island) and the north-western slopes of Taimyr (Sverdrup Island) and adjacent continental sections of the Taimyr Peninsula. In these areas meaning of heat flux is about 50 mW / m². Thus, the relationship between the magnitude of the heat flux

and the age of the cortex is revealed. As the crust becomes more ancient, eastward, in the direction of the Siberian platform, the heat flux decreases (Khutorskoy et al. 2013).

The shelf part of the Laptev Sea is poorly studied geothermally. The Laptev Sea shelf, located on the continental margin, to which the spreading axis of the Eurasian basin of the Arctic Ocean orthogonal approaches, has a typical structure for the edge margins. The Laptev megarift has internal grabens and horst and terraced boards. Active mid-ocean ridges approach the edges of continents, in addition to the Laptev Sea, only in the region of the Gulf of California in the Pacific Ocean and in the Gulf of Aden in the Indian Ocean (Khutorskoy et al. 2013). The active mid-oceanic ridge of Gakkel and the ocean basins of Nansen and Amundsen divided by it are orthogonal to the continental slope. A completely different nature of heat flow is observed on the Gakkel Ridge, the spreading ridge of the Arctic Ocean. Here it is quite high (more than 100 mW / m²), despite the slow speed of spreading (Andieva 2008).

Quite limited data about thermal regime of sediments in the Arctic Ocean make it difficult to define precise meaning of geothermal gradient for the areas of research of this master thesis. Thus, for calculation in this research next meaning of geothermal gradient were taken:

- for Kara sea: 3 ° C per 100 meters as average meaning of geothermal gradient
- for Laptev sea: 4,2⁰ C per 100 meters. It was counted as proportion in comparison with geothermal gradient in Kara Sea and according to approximate meaning of heat fluxes in Kara Sea as 70 mW / m² and in Laptev Sea 100 mW / m². As it was mentioned, we take geothermal gradient in Laptev Sea higher than average because of closeness of Gakkel ridge with higher heat fluxes.

3.2 Methane fluxes

3.2.1 Organic carbon content

The ocean presents all the main native types of carbon compounds (organic, inorganic) and forms of existence in the environment. Total Organic Carbon (Corg) in Oceans, enclosed in biota and inanimate matter, estimated at $4 * 10^{15}$ and $1100 * 10^{15}$ gramm, respectively. Organic carbon is mainly presented by next forms: dissolved (particles less than 1 nm), colloidal, including nanosystems (1-10 nm), highly dispersed structures (10-1000 nm), coarse colloids (1-100 microns) and suspended organic matter

(usually particles greater than 0.45 microns) and bottom sediments, silt water, gas hydrates (Romankevich et al. 2009).

The main primary source of organic matter in the ocean is phytoplankton, which annually creates $(70-103) \cdot 10^{15}$ g of Corg. Organic matter also can be produced by ice algae, phytobenthos ($0.6 \cdot 10^{15}$ g of Corg per year), which is created by macrophytes, diatoms living in silts, also chemolithotrophs in the rift zones of the ocean and in cold leaking out fluids, which are widely developed in the seas and on the periphery of all oceans (Romankevich et al. 2009).

Huge amount of the organic matter from land is brought with river runoff in dissolved ($210 \cdot 10^{12}$ g Corg per year) and suspended form ($370 \cdot 10^{12}$ g Corg per year) and its distribution in the ocean is very uneven. According to the recent studies, $27 \cdot 10^{12}$ g of Corg reach the Arctic Ocean annually with river runoff. The mixing zone, where the rivers flow into the ocean, has very important role in the deposition of different forms of organic matter, sorption of trace elements, and their distribution in the ocean. 40–90% of organic matter can settle in estuarine zones and on the adjacent shelf. However, over time, part of the sediments with organic matter influenced by gravity, tectonic movements or sea currents, can be transferred in the lower continental slope and its foot. This determines a high coefficient of organic matter fossilization on the continental margin of the oceans (Romankevich et al 2009).

According to Grigoriev et al. (2010) sediment flux to the Laptev Sea from the coastal sector - about 16×10^6 tons/year, organic carbon flux - about 0.3×10^6 tons/year.

According to Streletskaya et al. (2009) the coastal flux into the Kara Sea is 35 million tons. From this 27 million tons belongs to solid material, 7.6 million tons belongs to thawed ground ice, 0.4 million tons to organic carbon, and 0.3 million tons to soluble salts.

According to Romankevich (2015) organic carbon content varies from 0 to more than 2 % in Kara Sea with highest meaning near shore in delta areas. The same for Laptev Sea organic carbon content varies from 0 to more than 2 %. The map is presented on figure 14.

Based on the organic carbon content in bottom sediments theoretical amount of methane which can be generated by microbes can be calculated.

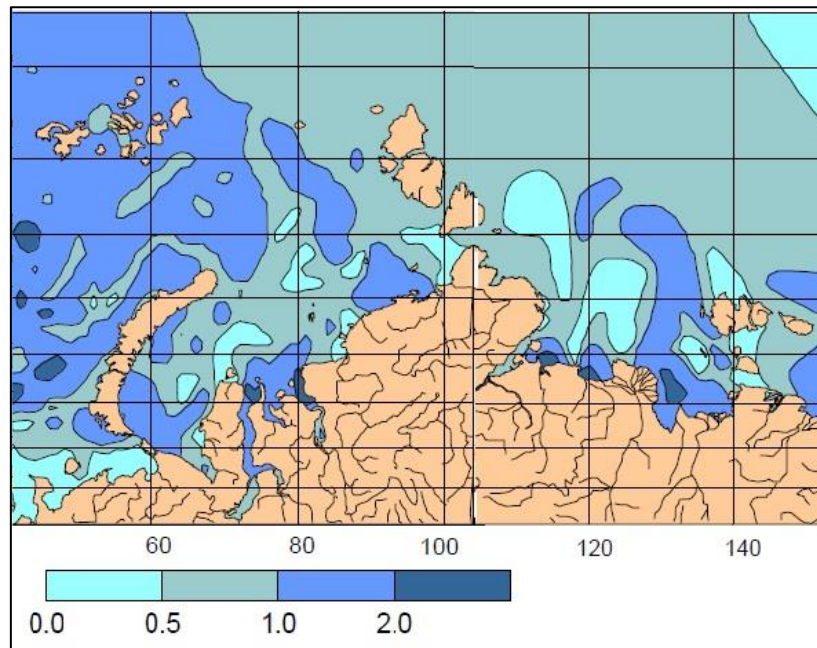


Figure.14 Organic carbon content (%) in bottom sediments of the Kara and Laptev Seas (Romankevich 2015)

3.6 Methane content

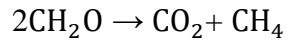
Methane in marine sediments can be generated either by cracking of complex organic molecules at great depths at the high temperatures conditions (thermogenic methane generated from the kerogen during the catagenesis) or by bacterial transformation of organic or inorganic carbon at shallower depths (microbial methane produced by archaea during the diagenesis) (James et al. 2016). The subaquatic appearance of gas hydrate deposits is facilitated by the widespread microbial generation of methane in bottom sediments. In order for the produced gas not to leave the sediments as a result of diffusion, a sufficient rate of its generation and, accordingly, a sufficient amount of organic matter buried in the sediments are necessary (Vorobyev, Malyukov 2009).

The general diagenetic zonation of sediments from top to bottom consists of three zones (Whiticar 1999):

- 1) the aerobic zone, where organic matter is oxidized (the conventional formula of organic matter is CH_2O) in the presence of free oxygen using aerobic bacteria.
- 2) anaerobic oxidation zone of organic matter and methane through sulfate reduction, where microbes are the driving force.
- 3) anaerobic methane formation zone

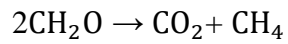
Methane is generated in the third anaerobic methane formation zone due to the destruction of organic matter by bacteria (Whiticar 1999).

The overall methane generation reaction in this zone is:



According to the reaction, one mole of CO_2 and one mole of CH_4 are obtained from two moles of organic matter (CH_2O).

According to the molar mass, this reaction can be written as follows:



$$60 \text{ g / mol} \rightarrow 44 \text{ g / mol} + 16 \text{ g / mol}$$

Based on this reaction, the amount of methane can be calculated by stoichiometric method.

4. Results

In this research it was decided to determine where gas hydrates can lay directly near the bottom surface in the Kara Sea and the Laptev Sea. After that, potential methane fluxes were estimated.

Calculations were done for submeridional and sublatitudinal profiles in the Kara and Laptev Seas (figure 15). Submeridional and sublatitudinal sections are shown on the figure. Points of the profiles are taken from different depths of the Kara and Laptev Seas shelves. The map was created based on isobaths from GEBCO and then edited in Global Mapper and graphical redactor.

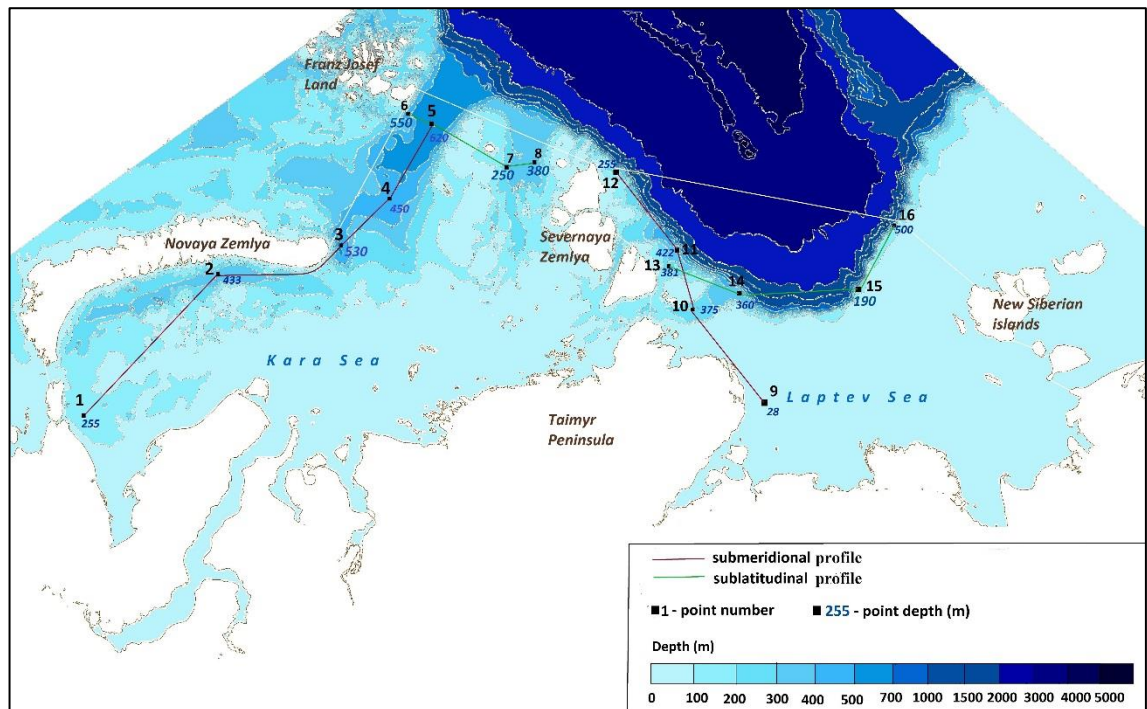


Fig. 15. Submeridional and sublatitudinal profiles in the Kara and Laptev Seas

4.1 Gas hydrates stability zone

Calculations were done for four gas mixtures in gas hydrates:

- 100% methane;
- 99% methane and 1% ethane;
- 95% methane and 5% ethane;
- 90% methane and 10% ethane.

Calculations for four gas mixtures in gas hydrates for submeridional and sublatitudinal sections in the Kara and Laptev Seas are represented below. Meanings of bottom temperature and bottom salinity are taken from maps of previous chapters. Equilibrium pressure were calculated with the program Hydoff (Hydrate prediction program) program.

Kara Sea (submeredional section)

Submeredional section in the Kara Sea consists of 5 point with depth from 255 m to 620 m. Temperature of bottom sediments are negative in all points (from -1.75 to -1 C°). Bottom salinity in all point are similar (from 34.4 to 34.6 ‰). Tables with calculations for four gas mixtures in gas hydrates are given below.

Based on the calculations for gas hydrate with 100 % of methane (table 1) the top of gas hydrates stability zone is located below the bottom surface only in point № 1. In other points calculated depth of GHSZ's top is located above the seafloor. How it was mentioned in the chapter about the concept of gas hydrate stability zone, the ocean water does not contain enough gas to stabilise hydrate and normally for marine settings the top of the GHSZ is defined at the sea floor (Amundsen, Martin 2012).

Table 1. Gas hydrate stability with 100% methane

Point №	Point's depth, m	T, C°	T, K	Salinity, ‰	P, kPa	Calculated depth of GH, m
1	255	-1,75	271.4	34,4	2560.642	261,1
2	433	-1,75	271.4	34,6	2562.748	261,3
3	530	-1	272.15	34,3	2746.976	280,1
4	450	-1,5	271.65	34,3	2620.530	267,2
5	620	-1,5	271.65	34,4	2621.610	267,3

For gas hydrate with 99% of methane and 1 % of ethane (table 2) top of GHSZ in all points are located above the seafloor, so gas hydrates in all points can reach the bottom surface.

Table 2. Gas hydrate stability with 99% methane and 1% ethane

Point №	Point's depth, m	T, C°	T, K	Salinity, ‰	P, kPa	Calculated depth of GH, m
1	255	-1,75	271.4	34,4	2384.300	243,1
2	433	-1,75	271.4	34,6	2386.268	243,3
3	530	-1	272.15	34,3	2560.724	261,1
4	450	-1,5	271.65	34,3	2440.996	248,9
5	620	-1,5	271.65	34,4	2441.998	249

The same, for gas hydrate with 95% of methane and 5 % of ethane (table 3) top of GHSZ in all points are above the seafloor, and gas hydrates in all points reach the bottom surface.

Table 3. Gas hydrate stability with 95% methane and 5% ethane

Point №	Point's depth, m	T, C°	T, K	Salinity, ‰	P, kPa	Calculated depth of GH, m
1	255	-1,75	271.4	34,4	1876.973	191,4
2	433	-1,75	271.4	34,6	1878.533	191,6
3	530	-1	272.15	34,3	2021.603	206,1
4	450	-1,5	271.65	34,3	1923.422	196,1
5	620	-1,5	271.65	34,4	1924.223	196,2

For gas hydrate with 90% of methane and 10% of ethane (table 4) gas hydrates in all points are located near the bottom surface also.

Table 4. Gas hydrate stability with 90% methane and 10% ethane

Point №	Point's depth, m	T, C°	T, K	Salinity, ‰	P, kPa	Calculated depth of GH, m
1	255	-1,75	271.4	34,4	1495.877	152,5
2	433	-1,75	271.4	34,6	1497.126	152,7
3	530	-1	272.15	34,3	1613.690	164,4
4	450	-1,5	271.65	34,3	1533.720	156,4
5	620	-1,5	271.65	34,4	1534.351	156,5

We can see that with rising of ethane content in gas mixture in gas hydrate the depth of GHSZ is becoming lower.

Further the thickness of the gas hydrate stability zone (top and base) was calculated. The table with calculations of base and thickness of GHSZ for all points for all profiles are represented in attachment 1.

Below graphs of GHSZ for four gas mixtures in gas hydrates for all points in submeredional section in the Kara Sea are represented. Top of GHSZ were defined above in the Hydoff program. We concluded that if the top of GHSZ calculated in Hydoff is located above the seafloor, we take the depth of the seafloor as the top of GHSZ. Geothermal gradient for Kara Sea was defined as 3 ° C per 100. This allows us to find the base of the GHSZ and then calculate the thickness of the GHSZ.

GHSZ for four gas mixtures in gas hydrates for five points of submeredional section in the Kara Sea are shown on the graphs in figure 16.

Point 1 has the lowest depth of 255 m. For gas hydrate with 100% methane the top of GHSZ are located below the seafloor. In our research we are interested only in those cases where gas hydrates reach the seafloor. Gas hydrates with admixture of ethane reach the seafloor. From graph we can see that than more ethane content in gas hydrate than deeper the base of GHSZ.

For point 1 base of GHSZ varied from 586 m for gas hydrate composed with 99% of methane and 1 % of ethane to 790 m for mixture 90% of methane and 10% of ethane. Thickness of GHSZ changed respectively, than more ethane content in gas hydrate than more thickness of GHSZ. For point 1 it changed from 331 m for gas hydrate with 99% of methane and 1 % of ethane to 535 m for 90% of methane and 10% of ethane.

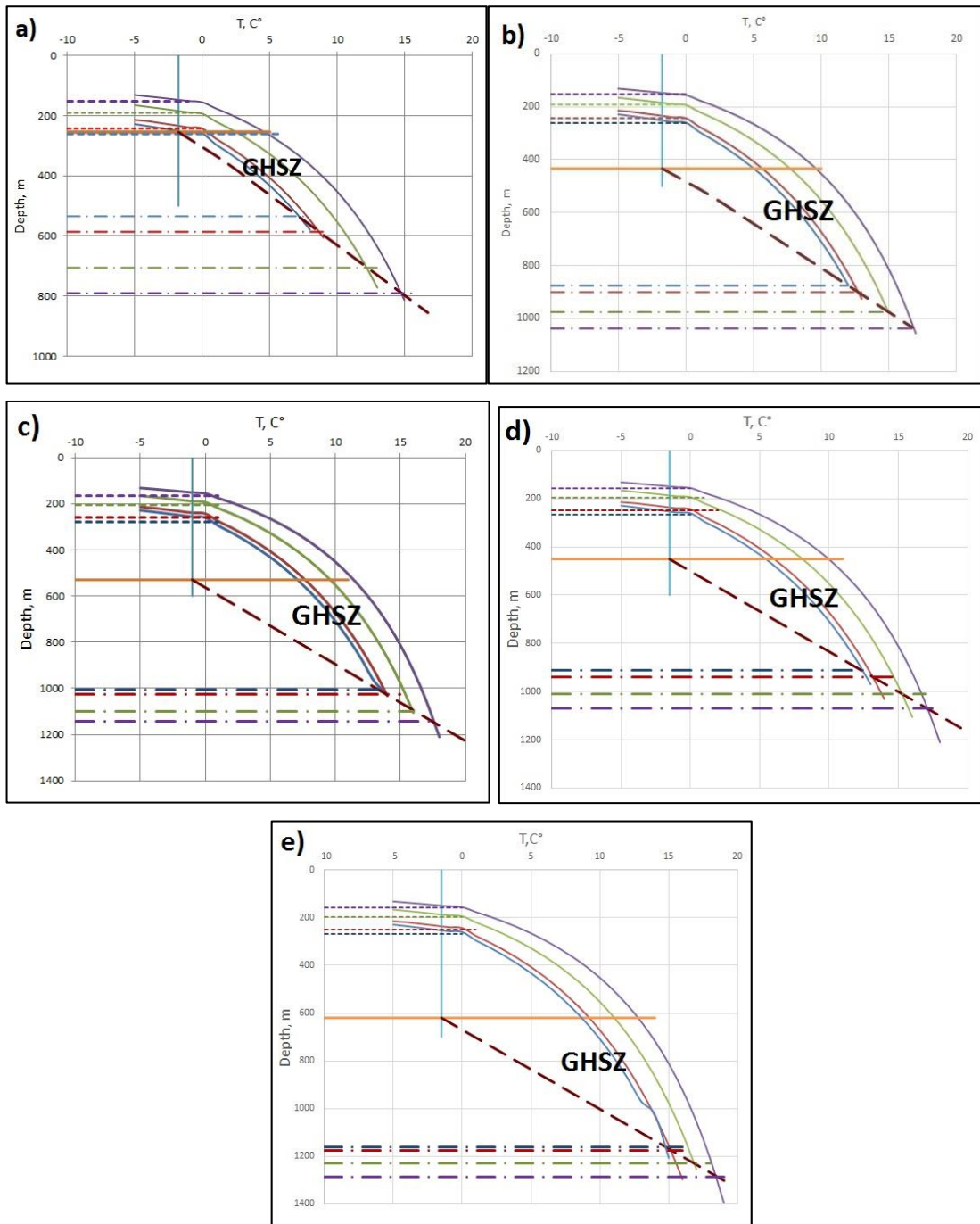
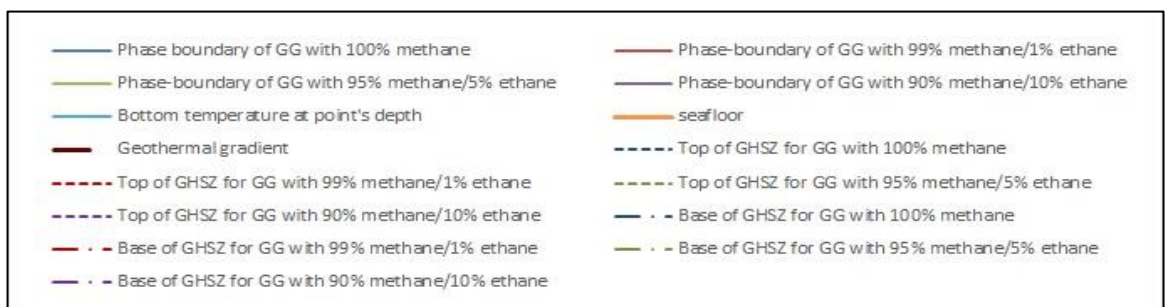


Figure 16. GHSZ for four gas mixtures in gas hydrates for submeredional section in the Kara Sea: a) point 1, b) point 2, c) point 3, d) point 4 e) point 5



For point 2 with depth of seafloor (equal to the top of GHSZ) at 433 m gas hydrates with all types of gas mixture reach the seafloor. Base of GHSZ changed from

875 m for gas hydrate with 100% of methane to 1037 m for gas hydrate with 90% of methane and 10% of ethane. Thickness of GHSZ varied respectively: from 422 m for gas hydrate with 100% of methane to 604 m for gas hydrate with 90% of methane and 10% of ethane.

For point 3 with depth of seafloor at 530 m gas hydrates with all types of gas mixture reach the seafloor. Base of GHSZ varied from 1005 m for gas hydrate with 100% of methane to 1145 m for gas hydrate with 90% of methane and 10% of ethane. Thickness of GHSZ changed from 475 m for gas hydrate with 100% of methane to 615 m for gas hydrate with 90% of methane and 10% of ethane respectively.

For point 4 with seafloor depth at 530 m gas hydrates with all types of gas mixture reach the seafloor. Base of GHSZ varied from 910 m to 1070 m for gas hydrate with 100% of methane and for gas hydrate with 90% of methane and 10% of ethane respectively. Thickness of GHSZ changed from 460 m to 620 m.

The point 5 has the deepest meaning of seafloor depth (620 m). Here base of GHSZ changed from 1160 m to 1285 m for gas hydrate with 100% of methane and for gas hydrate with 90% of methane and 10% of ethane. Thickness of GHSZ changed from 540 to 665 m respectively.

So, for submeridional sections of the Kara Sea the biggest thickness (665 m) is reached at point 5 with seafloor depth 620 m for gas hydrate with 90% of methane and 10% of ethane

In common we can conclude that gas hydrates which contain more percent of ethane have more extensive thickness. Also we can observe the trend that then deeper the seafloor then deeper the base of GHSZ and then more thickness of GHSZ. But it also depends from the meaning of bottom temperature and salinity. In the case for submeridional section of the Kara Sea these characteristics do not vary significantly.

Kara Sea (sublatitudinal section)

Sublatitudinal section in the Kara Sea consists of four points with depth from 250 m to 620 m. Tables with calculations for four gas mixtures in gas hydrates are given below.

For gas hydrate with content 100 % of methane (table 5) only in point 7 top of GHSZ is located below the seafloor. In other points gas hydrates with 100% methane reach the bottom surface.

Table 5. Gas hydrate stability with 100% methane

Point №	Point's depth, m	T, C°	T, K	Salinity, ‰	P, kPa	Calculated depth of GH, m
6	550	-1,5	271.65	34,5	2622.684	267,4
5	620	-1,5	271.65	34,4	2621.610	267,3
7	250	-0,5	272.65	34,4	2880.981	293,8
8	380	-1,25	271.9	34,4	2684.087	273,7

The same situation for gas hydrate with 99% methane and 1% ethane (table 6).

Gas hydrate in all points reach the bottom surface, except point 7.

Table 6. Gas hydrate stability with 99% methane and 1% ethane

Point №	Point's depth, m	T, C°	T, K	Salinity, ‰	P, kPa	Calculated depth of GH, m
6	550	-1,5	271.65	34,5	2443.012	249,1
5	620	-1,5	271.65	34,4	2441.998	249
7	250	-0,5	272.65	34,4	2687.699	274,1
8	380	-1,25	271.9	34,4	2501.154	255

For gas hydrate with 95% of methane and 5 % of ethane (table 7) top of GHSZ in all points are above the seafloor, and gas hydrates in all points reach the bottom surface.

Table 7. Gas hydrate stability with 95% methane and 5% ethane

Point №	Point's depth, m	T, C°	T, K	Salinity, ‰	P, kPa	Calculated depth of GH, m
6	550	-1,5	271.65	34,5	1925.024	196,3
5	620	-1,5	271.65	34,4	1924.223	196,2
7	250	-0,5	272.65	34,4	2125.871	216,8
8	380	-1,25	271.9	34,4	1972.709	201,5

Gas hydrates with 90% methane and 10% ethane (table 8) reach the bottom surface in all points.

Table 8. Gas hydrate stability with 90% methane and 10% ethane

Point №	Point's depth, m	T, C°	T, K	Salinity, ‰	P, kPa	Calculated depth of GH, m
6	550	-1,5	271.65	34,5	1534.995	156,5
5	620	-1,5	271.65	34,4	1534.351	156,5
7	250	-0,5	272.65	34,4	1699.914	173,3
8	380	-1,25	271.9	34,4	1573.844	160,5

Below on the figure 17 graphs of GHSZ for four gas mixtures in gas hydrates for all points in sublatitudinal section in the Kara Sea are represented.

For point 6 with seafloor depth at 550 m gas hydrates with all types of gas mixture reach the seafloor. Base of GHSZ varied from 1060 m to 1200 m for gas hydrate with 100% of methane and for gas hydrate with 90% of methane and 10% of ethane respectively. Thickness of GHSZ changed from 510 m to 650 m.

Point 5 is common for sublatitudinal and submeridional section.

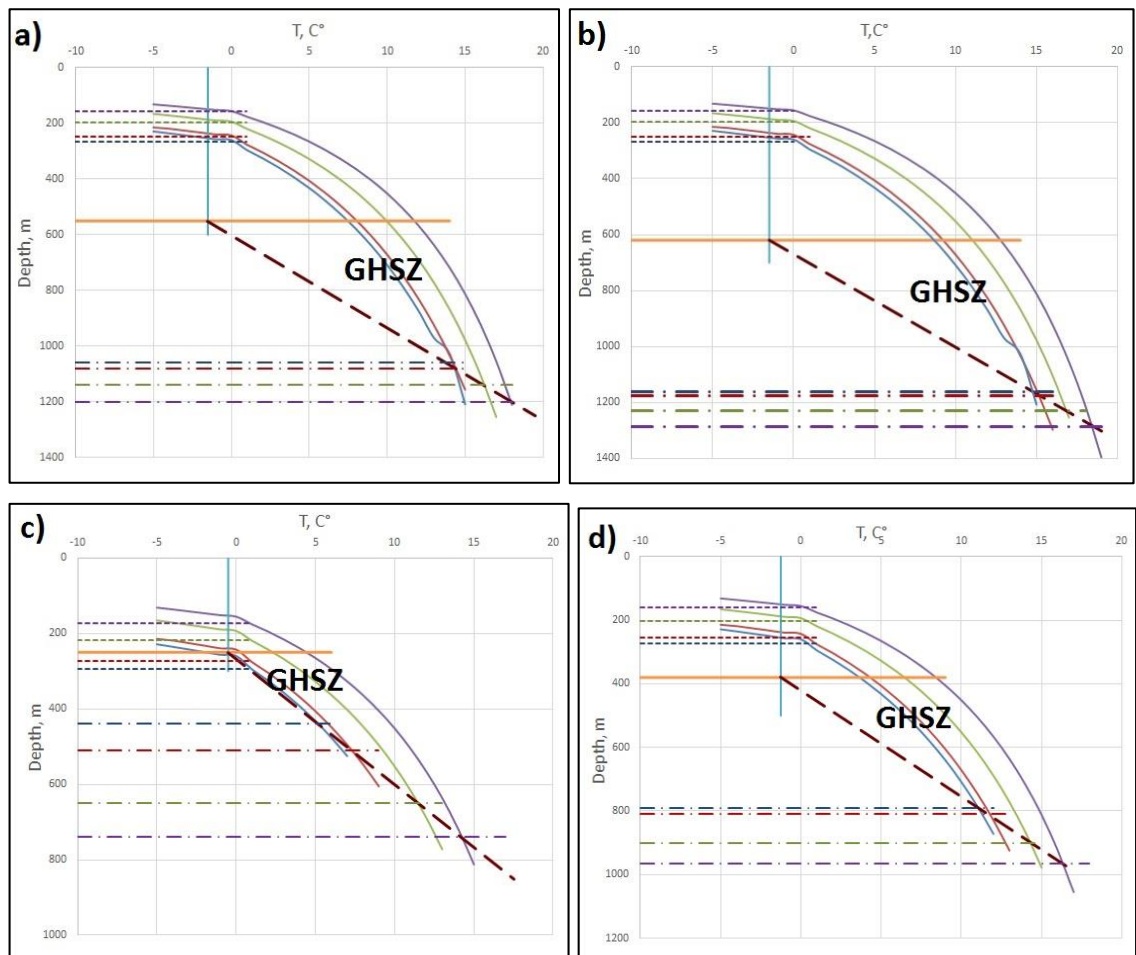
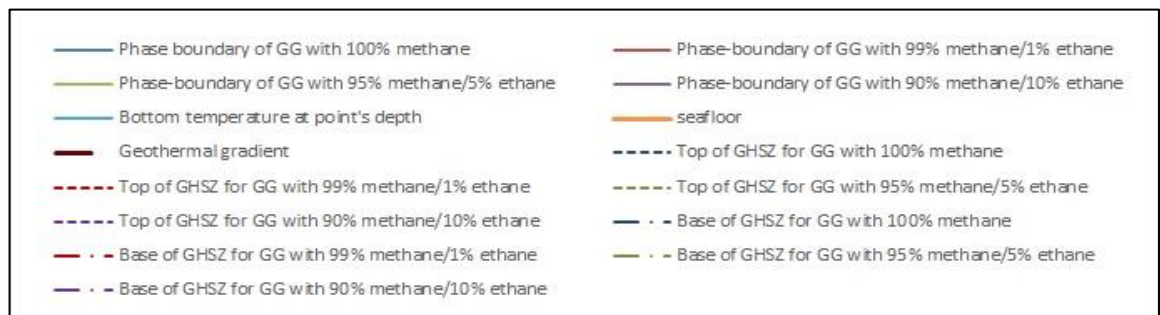


Figure 17. GHSZ for four gas mixtures in gas hydrates for sublittoral section in the Kara Sea: a) point 6, b) point 5, c) point 7, d) point 8



What relates to point 7 we can see from the graph that for gas hydrate with 100% of methane there is only weak intersection, so in this case we could say that the formation of gas hydrates in these conditions does not exist at any depth. Gas hydrates with 99% of methane and 1% of ethane do not reach the bottom surface. Gas hydrates with 95% of methane and 5% of ethane and with 90% of methane and 10% of ethane form GHSZ. Base of GHSZ varied from 650 m to 740 m and thickness of GHSZ from 400 to 490 m respectively.

For point 8 with seafloor depth at 380 m gas hydrates with all types of gas mixture reach the seafloor. Base of GHSZ varied from 790 m to 965 m for gas hydrate

with 100% of methane and for gas hydrate with 90% of methane and 10% of ethane. Thickness of GHSZ changed from 410 m to 585 m respectively.

For sublatitudinal section the biggest thickness of GHSZ is reached at point 5 with depth 620 m and for gas hydrate with 90% of methane and 10% of ethane.

Laptev Sea (submeredional section)

Submeredional section in the Laptev Sea consists of four points with depth from 28 m to 422 m. Tables with calculations for four gas mixtures in gas hydrates are given below.

For gas hydrate with content 100 % of methane (table 9) top of GHSZ is located below the seafloor in points 9 and 12. In points 10 and 11 gas hydrates with 100% methane reach the bottom surface.

Table 9. Gas hydrate stability with 100% methane

Point №	Point's depth, m	T, C°	T, K	Salinity, ‰	P, kPa	Calculated depth of GH, m
9	28	-1,75	271,4	33,5	2551.218	260,2
10	375	-1,5	271,65	34,3	2620.530	267,2
11	422	-0,75	272,4	34,3	2812.565	286,8
12	255	-1	272,15	34,4	2748.106	280,2

The same situation for gas hydrate with 99% methane and 1% ethane (table 10). Gas hydrate in points 9 and 12 do not reach the bottom surface. In points 10 and 11 top of gas hydrates is located above the seafloor.

Table 10. Gas hydrate stability with 99% methane and 1% ethane

Point №	Point's depth, m	T, C°	T, K	Salinity, ‰	P, kPa	Calculated depth of GH, m
9	28	-1,75	271,4	33,5	2375.481	242,2
10	375	-1,5	271,65	34,3	2440.996	248,9
11	422	-0,75	272,4	34,3	2622.875	267,5
12	255	-1	272,15	34,4	2561.790	261,2

Gas hydrates with 95% methane and 5% ethane (table 11) reach the bottom surface in all points, except point 9.

Table 11. Gas hydrate stability with 95% methane and 5% ethane

Point №	Point's depth, m	T, C°	T, K	Salinity, ‰	P, kPa	Calculated depth of GH, m
9	28	-1,75	271,4	33,5	1869.975	190,7
10	375	-1,5	271,65	34,3	1923.422	196,1
11	422	-0,75	272,4	34,3	2072.627	211,3
12	255	-1	272,15	34,4	2022.452	206,2

The same situation with gas hydrate with 90% methane and 10% ethane (table 12). Only in point 9 gas hydrates do not reach the bottom surface.

Table 12. Gas hydrate stability with 90% methane and 10% ethane

Point №	Point's depth, m	T, C°	T, K	Salinity, ‰	P, kPa	Calculated depth of GH, m
9	28	-1,75	271,4	33,5	1490.297	152
10	375	-1,5	271,65	34,3	1533.720	156,4
11	422	-0,75	272,4	34,3	1656.388	168,9
12	255	-1	272,15	34,4	1614.364	164.6

Below graphs with GHSZ for four gas mixtures in gas hydrates for all points in submeredional section in the Laptev Sea are represented (figure 18). Geothermal gradient for the Laptev Sea was defined as 4.2 ° C per 100 m.

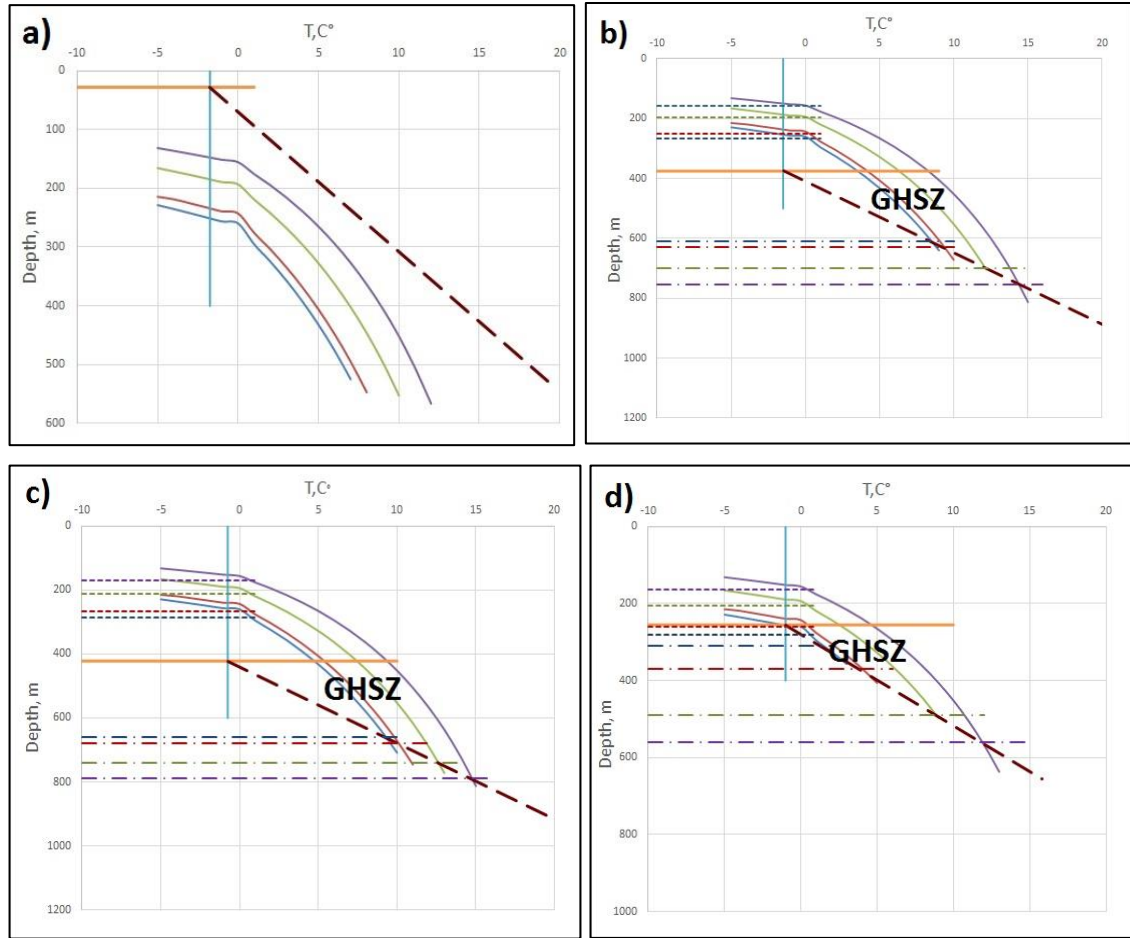
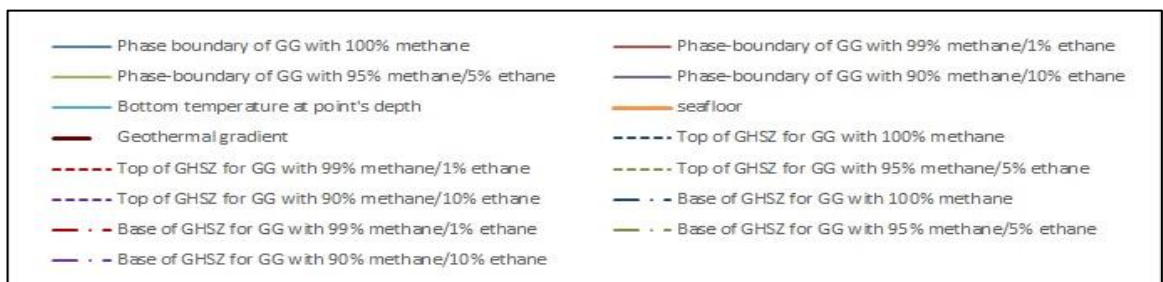


Figure 18. GHSZ for four gas mixtures in gas hydrates for submeredional section in the Laptev Sea: a) point 9, b) point 10, c) point 11, d) point 12



We can see from the graph that for point 9 with depth of seafloor of 28 m formation of gas hydrates at any depth is impossible for all types of gas hydrates, because there is no intersections between phase-boundary lines with geothermal gradient.

For point 10 with seafloor depth at 375 m gas hydrates with all types of gas mixture reach the seafloor. Base of GHSZ varied from 610 m to 755 m for gas hydrate with 100% of methane and for gas hydrate with 90% of methane and 10% of ethane. Thickness of GHSZ changed from 235 m to 380 m respectively.

For point 11 with depth of seafloor at 422 m the same, gas hydrates with all types of gas mixture can reach the seafloor. Base of GHSZ changed from 660 m for gas hydrate with 100% of methane to 790 m for gas hydrate with 90% of methane and 10% of ethane. Thickness of GHSZ varied from 238 m to 368 m respectively.

In the case of point 12 for gas hydrate with 100% of methane we can see only weak intersection, so in this case we could say that gas hydrates do not form at any depth. Gas hydrates with 99% of methane and 1% of ethane do not reach the bottom surface. Gas hydrates with 95% of methane and 5% of ethane and with 90% of methane and 10% of ethane form GHSZ. Base of GHSZ varied from 490 m to 560 m and thickness of GHSZ from 235 to 305 m respectively.

The biggest thickness of GHSZ is observed for point 10 (380 m) with seafloor depth 375 m and for gas hydrate with 90% of methane and 10% of ethane. Here we can see that point 11 (seafloor depth is 422 m) is deeper than point 10 (seafloor depth – 375 m), but in this case bottom temperature had influence and decreased meaning of base of GHSZ for point 11.

Laptev Sea (sublatitudinal section)

Sublatitudinal section in the Laptev Sea consists of four points with depth from 190 m to 500 m. Tables with calculations for four gas mixtures in gas hydrates are given below.

For gas hydrate with 100 % of methane (table 13) gas hydrates do not reach the bottom surface only in point 15 with depth of seafloor at 190 m. In the cases of other points top of the GHSZ are located above the seafloor.

The same situation is observed for gas hydrate with 99% methane and 1% ethane (table 14). Gas hydrate do not reach the bottom surface only in point 15.

Table 13. Gas hydrate stability with 100% methane

Point №	Point's depth, m	T, C°	T, K	Salinity, ‰	P, kPa	Calculated depth of GH, m
13	381	-1	272,15	34,3	2746.976	280.1
14	360	-1,5	271,65	34,3	2620.530	267.2
15	190	-1,5	271,65	34,2	2619.455	267.1
16	500	-1	272,15	34,1	2744.709	279,9

Table 14. Gas hydrate stability with 99% methane and 1% ethane

Point №	Point's depth, m	T, C°	T, K	Salinity, ‰	P, kPa	Calculated depth of GH, m
13	381	-1	272,15	34,3	2560.724	261.1
14	360	-1,5	271,65	34,3	2440.996	248.9
15	190	-1,5	271,65	34,2	2443.012	249.1
16	500	-1	272,15	34,1	2558.601	260.9

The situation for gas hydrate with 95% methane and 5% ethane (table 15) is similar to previous one.

Table 15. Gas hydrate stability with 95% methane and 5% ethane

Point №	Point's depth, m	T, C°	T, K	Salinity, ‰	P, kPa	Calculated depth of GH, m
13	381	-1	272,15	34,3	2021.603	206.1
14	360	-1,5	271,65	34,3	1923.422	196.1
15	190	-1,5	271,65	34,2	1922.623	196
16	500	-1	272,15	34,1	2019.911	206

Table 16. Gas hydrate stability with 90% methane and 10% ethane

Point №	Point's depth, m	T, C°	T, K	Salinity, ‰	P, kPa	Calculated depth of GH, m
13	381	-1	272,15	34,3	1613.690	164,6
14	360	-1,5	271,65	34,3	1533.720	156,4
15	190	-1,5	271,65	34,2	1533.079	156.3
16	500	-1	272,15	34,1	1612.347	164.4

Gas hydrates with 90% methane and 10% ethane (table 16) reach the bottom surface in all points.

Below on figure 19 graphs with GHSZ for four gas mixtures in gas hydrates for all points in sublatitudinal section in the Laptev Sea are represented.

For point 13 with depth of seafloor at 381 m, gas hydrates with all types of gas mixture can reach the seafloor. Base of GHSZ changed from 600 m for gas hydrate with 100% of methane to 745 m for gas hydrate with 90% of methane and 10% of ethane. Thickness of GHSZ varied from 219 m to 364 m respectively.

Gas hydrates in point 14 with seafloor depth at 360 m reach the seafloor for all types of gas hydrates. Base of GHSZ changed from 595 m to 735 m for gas hydrate with 100% of methane and for gas hydrate with 90% of methane and 10% of ethane respectively. Thickness of GHSZ varied from 235 m to 375 m.

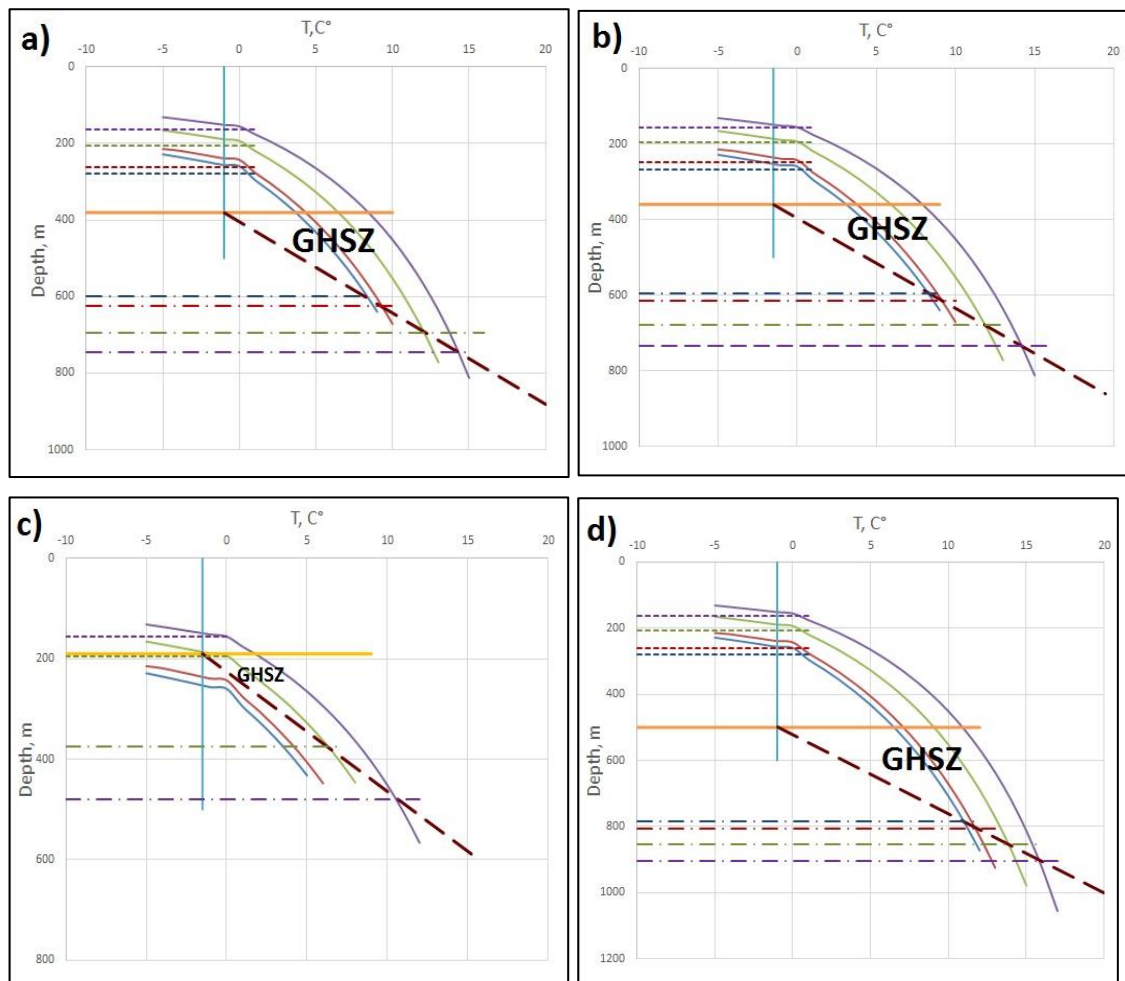
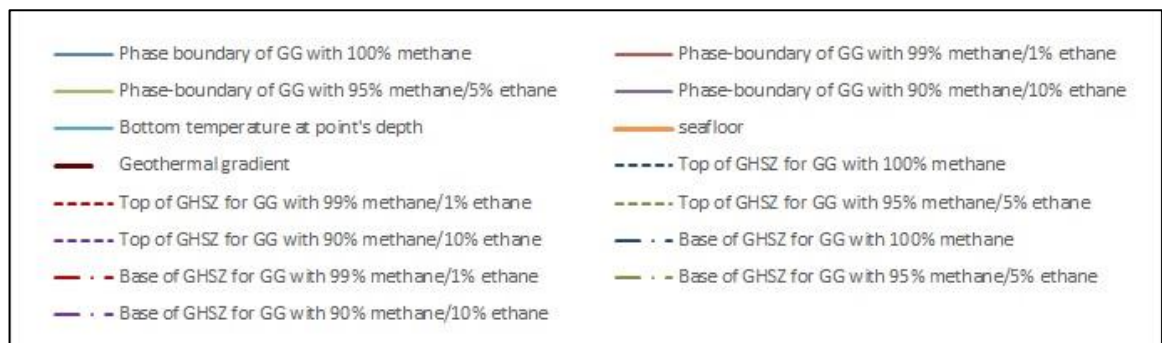


Figure 19. GHSZ for four gas mixtures in gas hydrates for sublittoral section in the Laptev Sea: a) point 13, b) point 14, c) point 15, d) point 16



As we can see from the graph of point 15 with sea floor depth 190 m for gas hydrates with 100 % of methane and with 99 % of methane and 1% of ethane GHSZ does not form at any depth. For gas hydrates with 95 % of methane and 5% of ethane base of GHSZ is located below the sea floor. For gas hydrates with 90 % methane and 10 % ethane GHSZ formed with base at 480 m. Thickness of GHSZ is 290 m.

Gas hydrates in point 16 with sea floor depth at 500 m reach the sea floor for all types of gas hydrates. Base of GHSZ changed from 785 m for gas hydrate with 100% of

methane to 905 m for gas hydrate with 90% of methane and 10% of ethane. Thickness of GHSZ varied from 285 m to 405 m respectively.

The biggest thickness of GHSZ (405 m) is reached in point 16 with seafloor depth 500 m and gas hydrate with 90% of methane and 10% of ethane.

Overall, we can conclude that then more ethane content in gas hydrate then thicker GHSZ can be formed. It also depends from the depth of the seafloor at concrete point, meanings of bottom temperature, bottom salinity and geothermal gradient.

We can see that gas hydrates can not be formed at shallow depth, for example in our research case at depth 28 m it is impossible for gas hydrates for all types of gas mixture. At depth 190 m gas hydrates can be formed and reach the seafloor only for gas hydrate with 90 % of methane and 10 % of ethane. Gas hydrates which contain at least 1 % of ethane in gas mixture can reach the bottom surface from meanings of seafloor depth around 255 m (for example point 1). Gas hydrates with 100 % of methane in our research need deeper depth of seafloor to form stable hydrates which can reach the bottom surface (more than 260 m depending from conditions). We have to take in account bottom temperature, bottom salinity and geothermal gradient which can change the thickness of GHSZ and its top and base.

Below the graphs (figures 20, 21, 22, 23) with change in thickness of GHSZ on four profiles are represented.

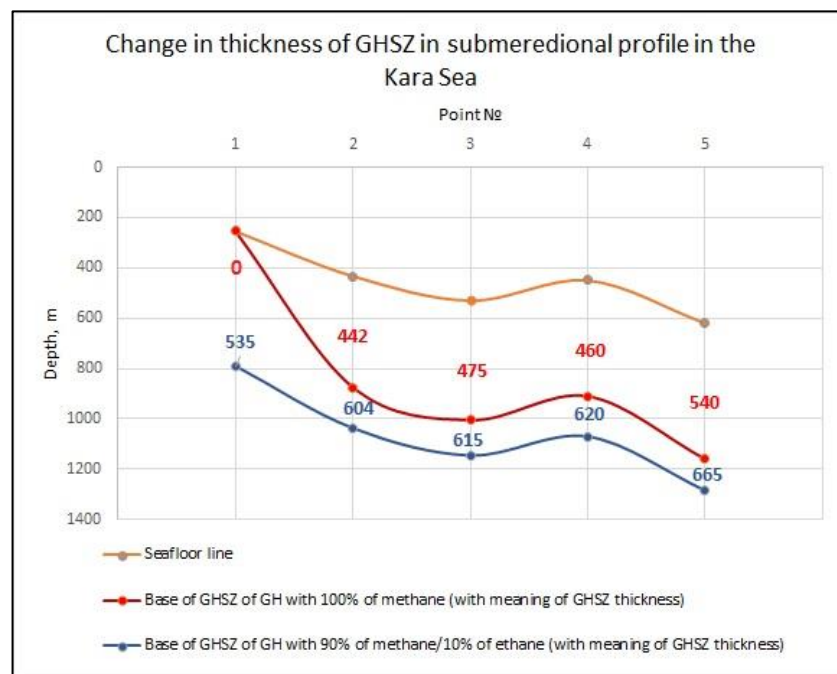


Figure 20. Change in thickness of GHSZ in submeredional profile in the Kara Sea.

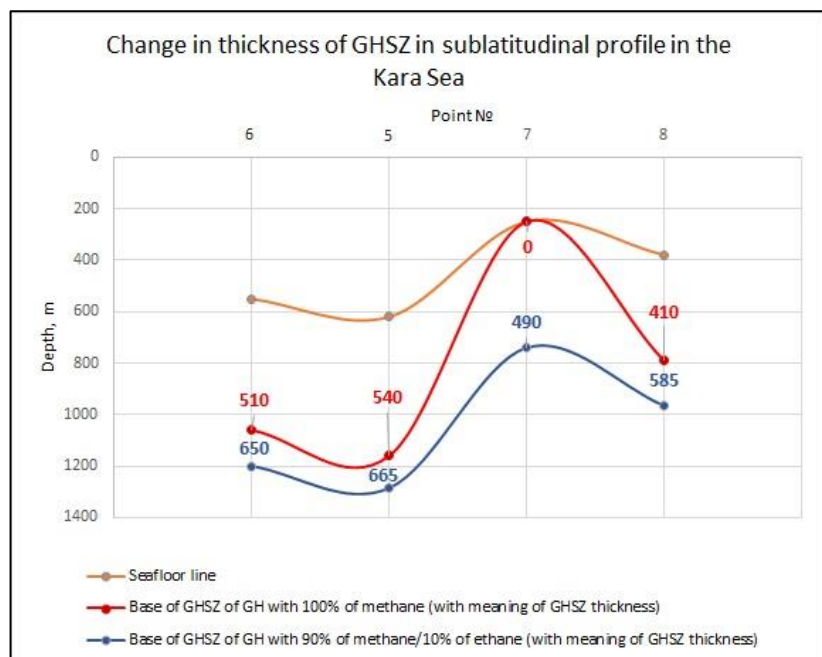


Figure 21. Change in thickness of GHSZ in sublatitudinal profile in the Kara Sea.

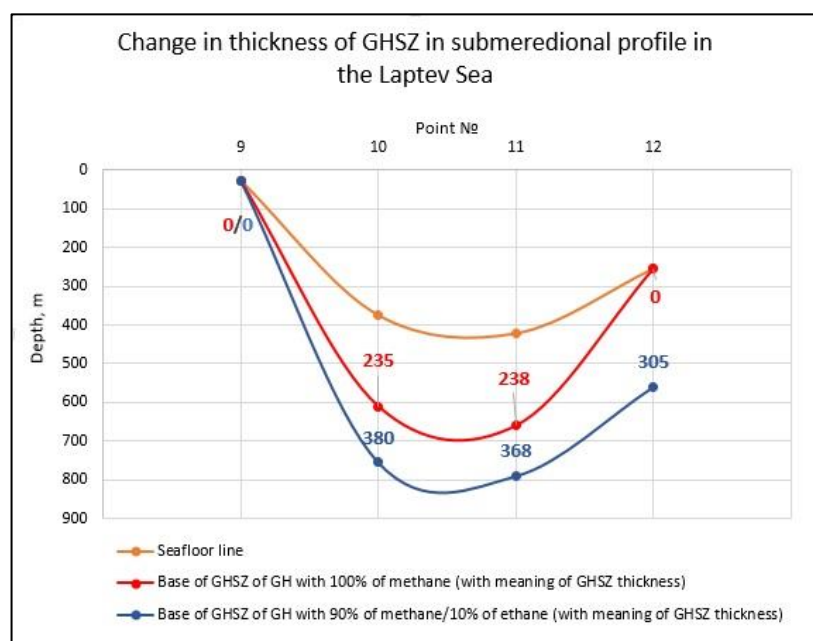


Figure 22. Change in thickness of GHSZ in submeridional profile in the Laptev Sea.

By red line the base of GHSZ of gas hydrates composed with 100 % of methane is shown. The blue line shows the base of GHSZ of gas hydrates composed with 90 % of methane and 10 % of ethane. The red and blue digits are the meaning of thickness of GHSZ for two composition of gas hydrates. Based on that graphs the differences in thickness of GHSZ between gas hydrates with 100% of methane and gas hydrates with 90% of methane and 10 % of ethane is about 150 m depending from the point.

11 points from 16 form GHSZ for gas hydrates composed of 100% of methane, and 15 points from 16 form GHSZ for gas hydrates composed of 90 % of methane and 10 % of ethane.

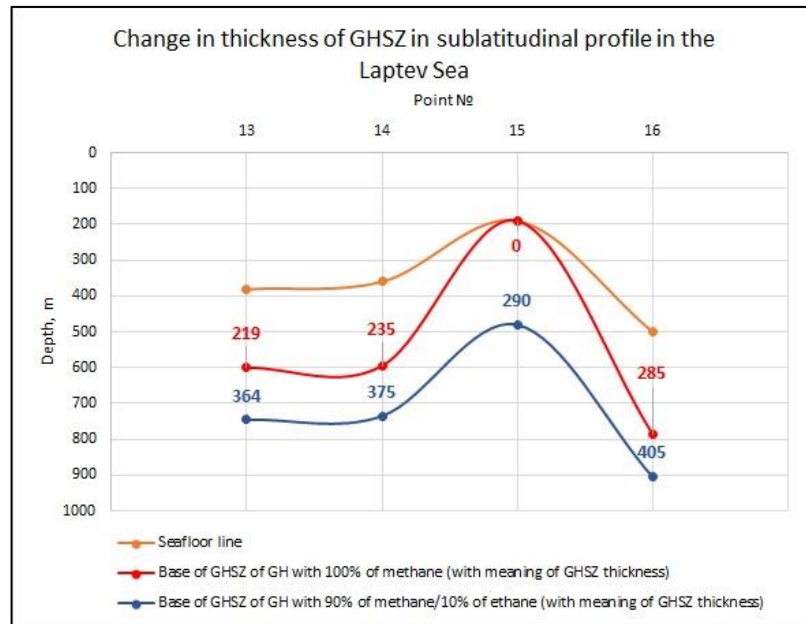


Figure 23. Change in thickness of GHSZ in sublatitudinal profile in the Laptev Sea.

If we compare thickness of GHSZ in Kara and Laptev Seas, we can see that GHSZ is thicker in the Kara Sea than in the Laptev Sea. The difference in thickness is about 200 m depending from the point. This fact can be explained that meaning of geothermal gradient is higher in the Laptev Sea. It can be concluded that, gas hydrates in the Laptev Sea are more vulnerable due to change of climatic conditions.

4.2 GHSZ during late Pleistocene

In late Pleistocene during the ice age (<21 ka) Arctic shelves were exposed to seawater regression (Serov et al. 2015) and subaerial conditions were established at the wide areas. Present water depths of ~120 m below sea level were drained (Portnov et al. 2014), that allows a thick layer of gas hydrates and permafrost to be formed (Serov et al. 2015). After the Last Glacial Maximum (LGM) (about 19 ka) Arctic shelves were flooded during the ocean transgression (Serov et al. 2015).

In this chapter calculations of characteristics of GHSZ for gas hydrates composed of 100 % of methane for conditions of late Pleistocene will be done.

It was assumed that at late Pleistocen sea level were 100 m lower than at present time. For the time of sea regression an average surface temperature was assumed -15°C, as was proposed by Serov et al. (2015). Bottom water temperature were determined as

-1.75, the minimum temperature according to Soloviev et al. 1987. Bottom salinity 35 ‰ were taken.

Calculated characteristics of GHSZ for all points are presented in attachment 2.

Below on the graphs (figures 24, 25, 26, 27), we can observe how characteristics of GHSZ changed in present time compared to late Pleistocene.

The dark blue line shows the sea level at late Pleistocene. Seafloor is shown by orange line. Red dash line represents the base of GHSZ at present time, blue dash line - the base of GHSZ Late Pleistocene. The thickness of GHSZ for both cases are marked.

The case for submeridional profile in the Kara Sea is shown on figure 24. For point 1 GHSZ is not formed for both cases. For all other points base of GHSZ for case of present time lays deeper then those for Late Pleistocene. The thickness of GHSZ for chosen points at present time is a bit more extensive than at Late Pleistocene, since bigger pressure created because of higher water level. The difference in thickness of GHSZ changes between 10 m in point 5 to 50 m in point 4.

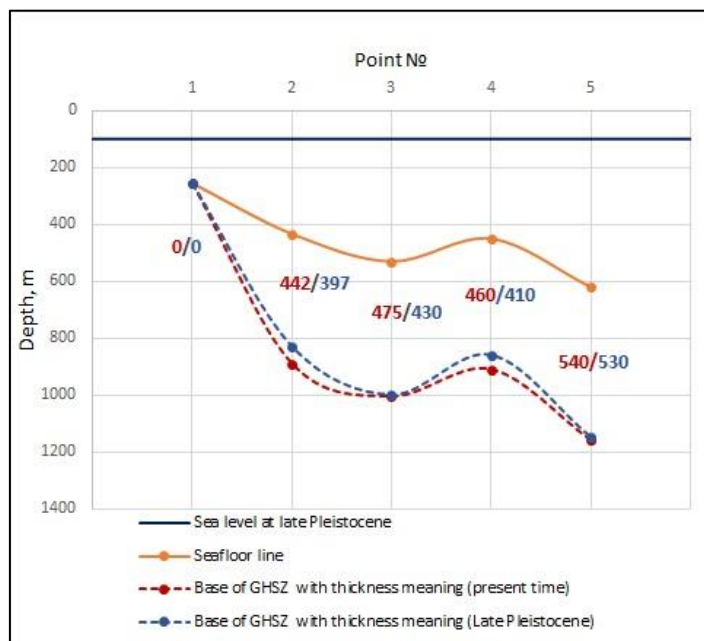


Figure 24. Characteristics of GHSZ in present time/Late Pleistocene in submeridional profile in the Kara Sea.

The case for sublatitudinal profile in the Kara Sea is shown on figure 25. GHSZ is not formed only in point 7 for both cases. For all other points the tendency is the same, base of GHSZ for case of present time is a bit deeper then those for Late Pleistocene. The difference in thickness of GHSZ changes between 10 m in point 5 to 60 m in point 8.

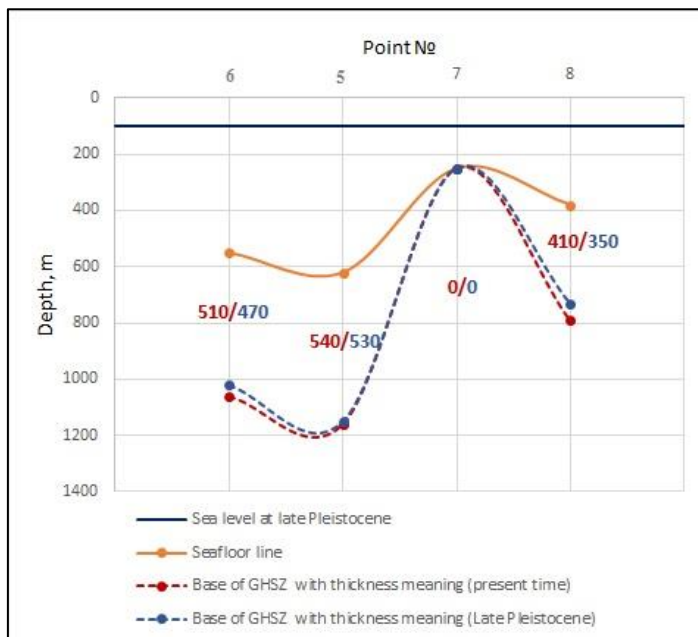


Figure 25. Characteristics of GHSZ in present time/Late Pleistocene in sublatitudinal profile in the Kara Sea.

The case for submeredional profile in the Laptev Sea is shown on figure 26. GHSZ is not formed in point 9 and 12 for both cases. The difference in thickness of GHSZ between two time periods varies from 70 m for point 10 to 30 m for point 11.

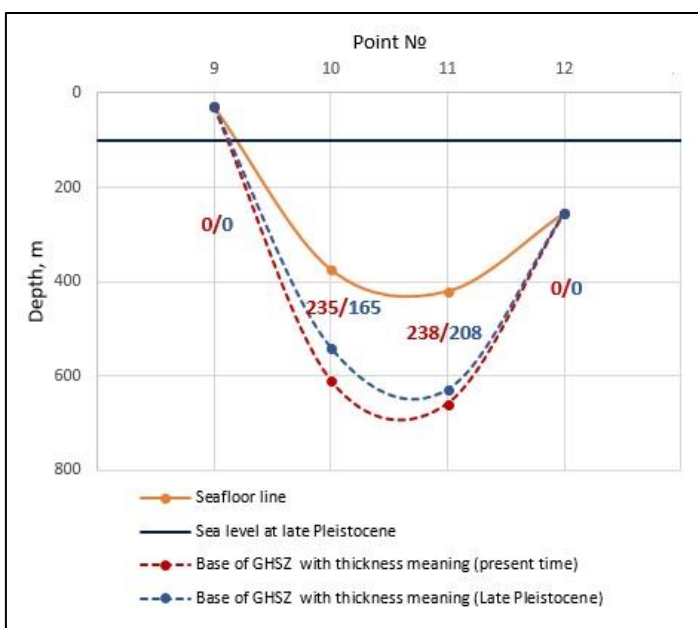


Figure 26. Characteristics of GHSZ in present time/Late Pleistocene in submeredional profile in the Laptev Sea.

The case for sublatitudinal profile in the Laptev Sea is shown on figure 27. GHSZ is not formed for point 15 in both cases. For the point 14 GHSZ, which can reach the bottom surface, is formed for the case at present time, but for Late Pleistocene

it does not form. The difference in thickness of GHSZ between two time period varies from 25 m for point 16 to 50 m for point 13.

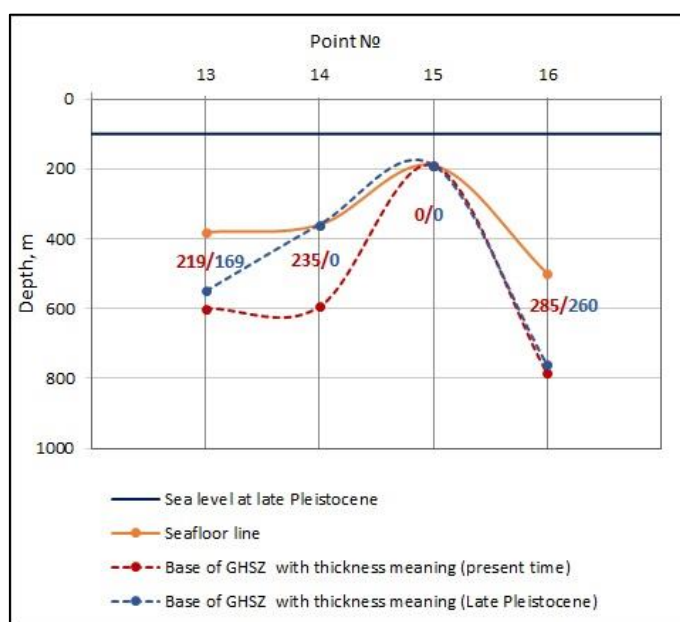


Figure 27. Characteristics of GHSZ in present time/Late Pleistocene in sublatitudinal profile in the Laptev Sea.

Overall, it can be concluded that GHSZ is thicker at present time than at Late Pleistocene because water level is now higher and it creates bigger pressure in spite of the fact that during Late Pleistocene the temperature was lower. The base of GHSZ of chosen points at present time is located a bit deeper than it was at late Pleistocene. The biggest difference in thickness of GHSZ is observed for points that located shallower, because the top of GHSZ is shifted more significant. For some of them the top goes deeper in sediments, or in some cases seafloor depth is too shallow to form GHSZ at all.

4.3 Methane fluxes

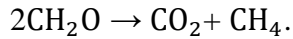
Microbes generate methane from organic matter in the diagenetic zone of methanogenesis: $2\text{CH}_2\text{O} \rightarrow \text{CO}_2 + \text{CH}_4$.

According on the content of organic carbon in bottom sediments we can calculate theoretical amount of methane which can be generated by microbes.

Corg (%) are taken from Romankevich (2015). Map of organic carbon content is presented in methodology chapter. According to the map of organic carbon content (%) for all points was defined. It varies from 0.5 to 2%. Meaning of Corg (%) are given in the table.

According to the reaction, one mole of CO_2 and one mole of CH_4 are obtained from two moles of organic matter (CH_2O).

According to the molar mass, this reaction can be written as follows:



$$60 \text{ g / mol} \rightarrow 44 \text{ g / mol} + 16 \text{ g / mol}$$

Based on that reaction next calculations were done: for bottom sediments with 0.5%, 1% and 2% of Corg respectively.

For Corg 0.5 % (or 5 g/kg)

Carbon

2 mol of CH_2O (60 g) contains: 24 g of C + 4 g of H + 32 g of O. Thus, the proportion of Corg in CH_2O will be 24 g/mol.

Then 5 g/kg of Corg will be equivalent to $5/24 = 0.21$ mol / kg in the molecule of organic matter (CH_2O).

Hydrogen

In organic matter (CH_2O) we have 4 g / mol of hydrogen.

An abstract sample of organic matter containing 0.5% Corg (or 5 g / kg), which is equivalent to 0.21 mol / kg, should also contain 0.21 mol / kg hydrogen based on stoichiometry. Thus $4 \text{ g / mol} * 0.21 \text{ mol / kg} = 0.84 \text{ g / kg}$ of hydrogen in the CH_2O molecule.

Oxygen

In organic matter (CH_2O) we have 32 g / mol of oxygen.

If we have 0.5% Corg (0.21 g / mol), then in this sample of organic matter there will be 0.21 mol of oxygen, that is $32 * 0.21 = 6.72 \text{ g / kg}$ of oxygen in the CH_2O molecule.

Thus, the mass of the CH_2O molecule for bottom sediments with a content of 0.5% Corg will be $5 + 0.84 + 6.75 = 12.56 \text{ g / kg}$

According to the reaction, at 0.5% Corg, the following amount of CO_2 and CH_4 will be released.

$$\text{CO}_2 = 44 * 0.21 = 9.24 \text{ g / kg} = 9240 \text{ ppm}$$

$$\text{CH}_4 = 16 * 0.21 = 3.36 \text{ g / kg} = 3360 \text{ ppm}.$$

If we check, whether the sum converges: $9.24 + 3.36 = 12.6 \text{ g / kg}$, which coincides with the calculation

For Corg 1% (or 10 g/kg)

Carbon

10 g of Corg will be equivalent to $10/24 = 0.42$ mol / kg in the molecule of organic matter (CH_2O)

Hydrogen

In organic matter (CH₂O) we have 4 g / mol of hydrogen.

An abstract sample of organic matter containing 1% Corg (or 10 g / kg) will contain $4 \text{ g / mol} * 0.42 \text{ mol / kg} = 1.68 \text{ g / kg}$ of hydrogen in the CH₂O molecule.

Oxygen

In organic matter (CH₂O) we have 32 g / mol of oxygen.

If we have 1% Corg (0.42 g / mol), then in this sample of organic matter $32 * 0.42 = 13.44 \text{ g / kg}$ of oxygen in the CH₂O molecule will be contained.

Thus, the mass of the CH₂O molecule for bottom sediments with a content of 0.5% Corg will be $10 + 1.68 + 13.44 = 25.12 \text{ g / kg}$

According to the reaction, at 1% Corg, the following amount of CO₂ and CH₄ will be released.

$$\text{CO}_2 = 44 * 0.42 = 18.48 \text{ g / kg} = 18480 \text{ ppm}$$

$$\text{CH}_4 = 16 * 0.42 = 6.72 \text{ g / kg} = 6720 \text{ ppm}$$

If we check, whether the sum converges:: $18.48 + 6.72 = 25.2 \text{ g / kg}$, which coincides with the calculation

For Corg 2% (or 20 g/kg)

Carbon

2 mol of CH₂O (60 g) contains: 24 g of C + 4 g of H + 32 g of O, that is, the proportion of Corg in CH₂O should be 24 g / mol.

Then 20 g of Corg will be equivalent to $20/24 = 0.83 \text{ mol / kg}$ in the molecule of organic matter (CH₂O).

Hydrogen

In organic matter (CH₂O) we have 4 g / mol of hydrogen.

An abstract sample of organic matter containing 2% Corg (or 20 g / kg) will contain $4 \text{ g / mol} * 0.83 \text{ mol / kg} = 1.68 \text{ g / kg}$ of hydrogen in the CH₂O molecule.

Oxygen

In organic matter (CH₂O) we have 32 g / mol of oxygen.

If we have 2% Corg (0.83 g / mol), then in this sample of organic matter $32 * 0.83 = 26.56 \text{ g / kg}$ of oxygen in the CH₂O molecule will be contained.

Thus, the mass of the CH₂O molecule for bottom sediments with a content of 2% Corg will be $20 + 3,32 + 26,56 = 49,88 \text{ g / kg}$

According to the reaction, at 2% Corg, the following amount of CO₂ and CH₄ will be released.

$$\text{CO}_2 = 44 * 0,83 = 36,52 \text{ g / kg} = 36520 \text{ ppm}$$

$$\text{CH}_4 = 16 * 0,83 = 13,28 \text{ g / kg} = 13280 \text{ ppm.}$$

If we check, whether the sum converges: $36,52 + 13,28 = 49,8 \text{ g / kg}$, which coincides with the calculation.

All calculated meanings are presented in attachment 3.

So, we can see than more organic carbon content in bottom sediments than more methane can be released. It is also interesting to notice significant amount of carbon dioxide, which can be generated together with methane. Its amount several times higher than amount of methane.

These calculated meanings of methane and carbon dioxide show the maximum possible amount of gas that can be generated by sediments. In reality, microbes never completely recycle Corg. Thus, if the actual gas content exceeds or close to the calculated, this means that there is an additional source of methane associated, for example, with the destruction of gas hydrates located deeper in the section.

According to field measurements performed in the Laptev Sea and the Kara Sea, the amount of methane in bottom sediments did not exceed 200 ppm accordong to unpublished data of FSBI “Vniiokeanologia”.

Thus, microbes during diagenesis recycle an insignificant part of Corg. The methane generated by archaea in the methane generation zone (zone 3) is probably almost completely oxidized in the sulfate reduction zone (zone 2). Therefore, the measured values of methane are much lower than those that we calculated.

Since measured values of methane is much lower than calculated it can be concluded that additional methane which can be generated by the destruction of gas hydrates is absent, at least at the points of this research.

So, thermobaric conditions are favorable for the formation of gas hydrates in most of the points of profiles. But their destruction in chosen points is not approved by our calculations. Thus, gas hydrates may exist at the area of this research, but now they are stable and do not have tendency to destruction. More complex research is needed to determine presence of gas hydrates in the region and their vulnerability to climate change.

5. Discussion

The most important findings from results chapter can be stated as follows:

- The thickness of GHSZ depends from composition of gas hydrates, seafloor depth, bottom temperature, bottom salinity and geothermal gradient
- Thermobaric conditions are favorable for the formation of gas hydrates in most of the points of profiles
- Than more content of ethane in gas hydrate, than lower the depth where it may exist
- Than more content of ethane in gas hydrate, than thicker the GHSZ
- Than lower the bottom temperature, than lower the depth where gas hydrates may exist
- Than lower bottom salinity, than lower the depth where gas hydrates may exist
- GHSZ is thicker at present time than at Late Pleistocene because water level is now higher and it creates bigger hydrostatic pressure.
- GHSZ in the Kara Sea is thicker than in the Laptev Sea, because geothermal gradient in Laptev Sea is higher. Bottom temperature and bottom salinity are quite similar in both cases.
- Destruction of gas hydrates in chosen points is not approved by calculations of amount of methane, which can be generated by bottom sediments. Gas hydrates may exist at the area of this research, but they do not have tendency to destruction.

Some of these findings have reflection by many authors in other research.

Giustiniani et al. (2013) suggests that gas hydrates reservoirs located in the Arctic can have significant impact on the amplification of climate changes and many efforts are needed to define the area of their distribution. Stability of gas hydrates is mainly defined by ocean permafrost/ bottom water temperature, meaning of geothermal gradient, water salinity, and gas composition. Presence of even insignificant percentage of some higher hydrocarbons (ethane or propane) can shifts the phase boundary to higher temperature. Thus the base of GHSZ will be shifted to greater depths at a given temperature (Giustiniani et al. 2013).

According to our calculations for gas hydrate with 100 % of methane to reach the seafloor we need seafloor depth more than 250 m. Gas hydrates with ethane content may exist at the lower depth around 160 m depending from conditions.

Bogoyavlensky et al. (2018) in their research about gas hydrates shows the cartographic diagram of the stability of methane hydrates in the Circumarctic region. On the figure 28 below we have cut fragment with Kara and Laptev Sea, where pink colored zones corresponds to zone of favorable thermobaric conditions, light green colored zones – to favorable zone of subaquatic permafrost, blue colored zones – to lack of conditions for the formation and the existence of the gas hydrates.

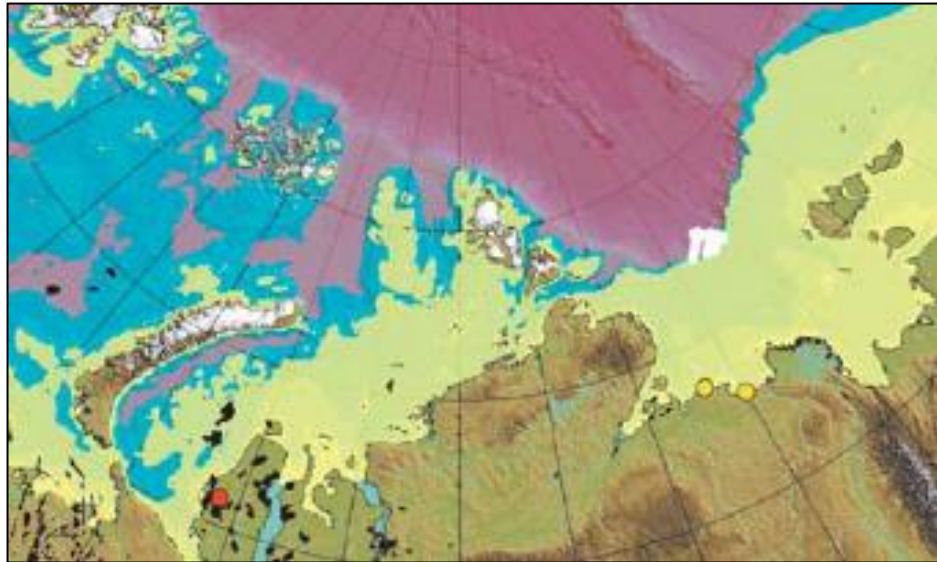


Fig. 28. Methane hydrate distribution in Kara and Laptev Seas (Bogoyavlensky et al. 2018)

According to this map zones of favorable thermobaric conditions relates to outer part of Laptev Sea shelf where it gradually deepening and goes into continental slope, and deeper part of the Kara Sea - St Anna Trough, Voronina Trough, Novaya Zemlya Trog. In common, it corresponds to my results that gas hydrates cannot reach the seafloor in shallow part of the shelf.

It should be noted that in addition to the zone of favorable thermobaric conditions for the modern formation and preservation of gas hydrates on the Arctic shelf, there is a region of the alleged development of subaquatic permafrost, which is a zone of gas hydrates metastability in which relic gas hydrates can be preserved due to the self-conservation effect (Bogoyavlensky et al. 2018). Zone of subaquatic permafrost is mostly corresponds to areas of shallow shelf, which does not have favorable thermobaric conditions. It means that zones of possible gas hydrates distribution can be more extensive. However, in this research area of subaquatic permafrost was not taken in account.

Klitzke et al. (2016) investigated gas hydrates stability zone in the Barents and Kara Seas for two different gas hydrates composition: pure methane and gas with composition of 90% of methane, 7% of ethane and 3 % of propane.

They proposed that gas hydrates which contain in their composition ethane, propane or other gases besides methane increase the stability of gas hydrates. Simulated thickness of GHSZ is shown on the figure 29 below.

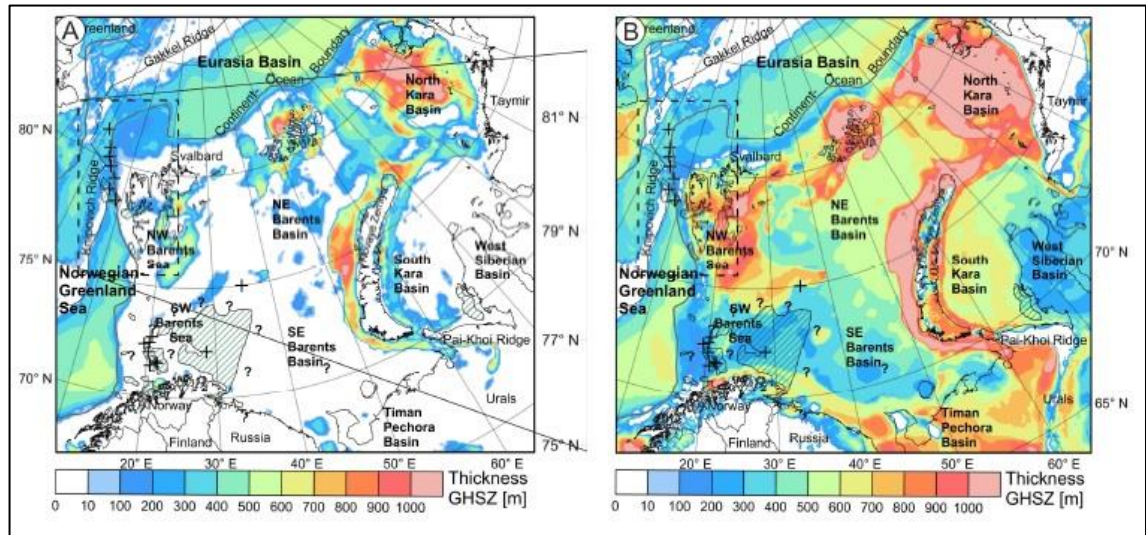


Fig. 29. Thickness of GHSZ: a) pure methane b) gas with composition of 90% of methane, 7% of ethane and 3 % of propane.

Stable pure methane hydrate is related only to areas with significant water depth and low meaning of geothermal gradient: near Novaya Zemlya, along the northern continental margin and in northern part of the Kara Sea. Methane hydrates with thickness of 100-300 meters are also stable locally in the central and eastern part of the Barents Sea and in the Timan Pechora Basin. Gas hydrates with composition of 90% of methane, 7% of ethane and 3 % of propane are potentially stable almost in the whole area. Maximal thickness of 1000 meters is observed in northern part of Kara Sea, near Franz Josef Land archipelago and from both sides of Novaya Zemlya. The remain part of the study area has the GHSZ thickness of 200 to 500 meters.

In my research there is the same tendency: the thickness of GHSZ become bigger with increase of ethane in hydrate composition. For example in my research in the Kara Sea the most extensive GHSZ relates to points in Novaya Zemlya trench and St Anna Trough with GHSZ thickness around 650 meters for gas hydrates with 90% of methane/10 % of ethane. In the research of Klitzke et al. (2016) thickness of GHSZ in these areas are around 1000 meters, but this differences can be explained by different

composition of gas hydrates and other characteristics for calculations: meaning of bottom temperature and geothermal gradient.

Evolution of submarine permafrost and GHSZ in the Laptev and East Siberian Sea shelf zones were studied by Romanovskii et al (2005). Eastern Siberian shelf has favorable conditions for formation of gas hydrates. Climate change and cycles of marine transgression-regression influence on thickness of permafrost and GHSZ. Because of sea level changes upper and lower boundaries of GHSZ may fluctuate. The marine transgression create additional pressure which equal to the seawater pressure at the seafloor. Opposite, the hydrostatic pressure decreases during ocean regressions. When modeled change of permafrost and GHSZ thickness during Quaternary researcher noticed that in the beginning of sea transgression permafrost was subjected to gradual degradation, whereas GHSZ was quite stable or even became thicker. This was caused by increase of water depth with following increase of hydrostatic pressure (Romanovskii et al 2005). That observation corresponds to my calculation of characteristics of GHSZ for late Pleistocene.

The methane emissions from shelf areas of the Arctic seas are expected due to high organic content of the sediments. Destabilization of gas hydrates deposits and enhanced methane release can be caused by increasing of ocean bottom temperature. Dissociated methane migrates from seafloor to water column and then release to the atmosphere. Now researchers observe increase methane emission into the atmosphere in the Arctic Region (Malakhova et al. 2018).

According to Malakhova et al. (2018) ocean areas with depth of 100 to 300 meters are subjected to significant methane emissions. A significant part of the methane emission from the seas occurs in the regions with a sea depth in the range from 100 to 300 m. The upper boundary of the gas hydrate stability zone there corresponds to depth of 250-300 meters, and increasing of bottom temperature may lead to dissociation of hydrates.

Malakhova et al. in their research estimated sensitivity of the gas hydrates stability in the Arctic ocean to the climate changes by the end of the 21st century. They were interested in zones of shallow and mid-depth shelf of the Arctic Ocean. Researchers proposed 6 models with different scenarios of warming: from small warming to very strong warming. Results of two models with small warming and very strong warming are shown on the figure 30.

As we can see the most significant increase of temperature is observed in Barents Sea, near Novaya Zemlya and Svalbard. It can be explained that this area is

under influence of warm Gulfstream. It is obvious that in this area we can expect the most intensive gas hydrates dissociation and methane release. In the scenario of strong warming Kara Sea is also subjected to rising of bottom water temperature. Laptev Sea has the weakest rising of bottom temperature.

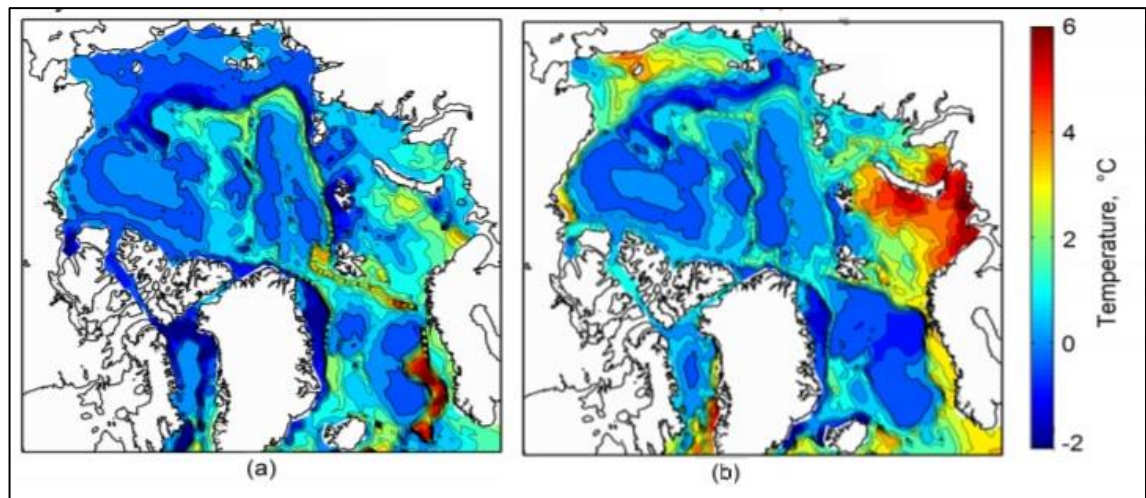


Figure 30. Bottom water temperature changes a) small warming b) very strong warming.

Methane release in the South Kara Sea were studied by Serov et al. (2015) from so-called pingo-like features (PLF), which represent seafloor doming formed after potential gas blowouts. Researchers have chosen two PLF: PLF 1 in Baydaratskaya Bay and PLF 2 near Novozemelsky Trough. In PLF 1 low-methane concentrations (14.2–55.3ppm) were observed. In contrast, PLF 2 demonstrates anomalously high concentrations of methane (>120,000ppm). It was hypothesized that the high concentrations of methane at PLF 2 can be explained by migration of methane of microbial origin from a deeper source.

In my case for chosen points additional methane source from gas hydrates was not detected. My calculated meanings of methane show the maximum amount of methane, which can be generated by microbes. Since lack of data about methane amount in bottom sediments in the region, my calculations were compared to average meaning of methane amount in bottom sediments (200 ppm) which is much lower than calculated.

It is important to understand that methane released from sediments is mitigated by several factors before it may reach the border of ocean-atmosphere system. The released methane may be dissolved in local pore waters, remain trapped as gas for example, may be consumed by anaerobic oxidation or oxidized by aerobic bacteria in water column. Only some percentage of methane generated by sediments can survives

during the trip through the water column and after reach the atmosphere (Giustiniani et al. 2013).

It should be noted that gas hydrates do not exist everywhere where there are favorable thermobaric conditions for formation and preservation, but only in certain areas and zones in which there is in situ gas or there is a gas inflow from the depths along faults, subvertical cracks, “gas pipes”, channels of mud volcanoes, etc (Bogoyavlensky et al. 2018). Thus, complex geological and geophysical research is needed to define the accurate existence of gas hydrates in certain area.

Conclusion

Gas hydrates contain huge amount of methane. Accept industrial potential, gas hydrates can play important role in climate change on global scale. Methane is very significant greenhouse gas, which is 25 time more effective than carbon dioxide. Methane release from gas hydrates may accelerate global warming and cause change in climate system. Especially it relates to Arctic region, where these changes are most noticeable.

Gas hydrate stability zone (GHSZ) is usually confined to areas of the ocean, including shelves and continental slopes. Thermobaric conditions for the formation of gas hydrates exist in most of the Arctic Ocean and in almost the entire Russian shelf of the Arctic.

In this research potential methane flux from gas hydrates distribution areas in the Kara and Laptev seas shelves were evaluated.

Calculations were done for two submeridional and two sublatitudinal profiles with 16 points in both seas.

Thickness of gas hydrate stability zone (GHSZ) were determined for 4 gas mixtures (GH with 100% of methane, GH with 99 % of methane and 1 % of ethane, GH with 95 % of methane and 5 % of ethane, GH with 90 % of methane and 10 % of ethane) in gas hydrates for each of the points. In this research only gas hydrates which lay directly near the bottom surface were taken in account.

It was concluded that than more content of ethane in gas hydrate than thicker the GHSZ and than lower the depth where it may exist. For example, the difference in thickness of GHSZ between gas hydrates with 100% CH₄ and gas hydrates with 90% CH₄ and 10% C₂H₆ is about 150 m. Gas hydrates with 90% CH₄ and 10% C₂H₆ may exist at the depth about 100 m shallower than gas hydrates with 100% CH₄. In our case 11 points from 16 form GHSZ for gas hydrates composed of 100% of methane, and 15 points from 16 form GHSZ for gas hydrates composed of 90 % of methane and 10 % of ethane.

The thickness of GHSZ depends from several characteristics: composition of gas hydrate, seafloor depth, bottom temperature, bottom salinity and geothermal gradient.

GHSZ in the Kara Sea is thicker than in the Laptev Sea, because geothermal gradient in Laptev Sea is higher. The difference in thickness of GHSZ is about 200 m depending from the point.

Present time conditions were compared with Late Pleistocene conditions to look how GHSZ can fluctuate with change of climate. Calculations of GHSZ characteristics

were made only for gas hydrates composed of 100 % of methane. According to calculations theoretically GHSZ is thicker at present time than at Late Pleistocene because water level is now higher and it create bigger hydrostatic pressure in spite of the fact that during Late Pleistocene the temperature was lower.

Potential methane flux was calculated based on organic carbon content in bottom sediments. The idea was to compare calculated meanings with real measurements, and if calculated meanings are close to calculated, it mean that there is additional source of methane from gas hydrate destruction. According to field measurements of FSBI Vniioekenologia in the Laptev Sea and the Kara Sea, average amount of methane in bottom sediments in the region did not exceed 200 ppm. Calculated meanings change from 6720 to 13280 ppm depending from content of organic carbon. These calculated values are much higher than measured in the field. It was concluded, that additional source of methane released from gas hydrates is absent, and so destruction of gas hydrates is not obserbed in chosen points.

Nevertheless, thermobaric conditions are favorable for the formation of gas hydrates in most of the points of profiles. But their destruction is not approved by our calculations. Theoretically, gas hydrates may exist at the area of this research, but now they are stable and do not have tendency to destruction.

More complex research is needed to determine presence of gas hydrates in the region and their vulnerability to climate change.

Acknowledgements

This Master Thesis is the result of the two year master program «Cold Region Environmental landscapes Integrated Science (CORELIS)» in the Institute of Earth Sciences in St. Petersburg State University.

I would like to say thanks to my scientific supervisor Dr. Alexey A. Krylov, Leading Reseacher in VNIIOkeangeologia and associate professor in St. Petersburg State University for his guidance and support during the writing of this Master Thesis. His feedback and comments were helpful and valuable to me.

I am grateful to the Department of the Geological mapping in FSBI "VNIIOkeangeologia", where I had my practice. There I collected some theoretical material for my research and got access to special program such as Hydoff (Hydrate prediction program), which helped me to make necessary calculations.

I also want to thank my scientific consultant Pavel Serov, PhD, VISTA postdoc at CAGE - Centre for Arctic Gas hydrate from The Arctic University of Norway for his valuable comments and feedback.

References

ACIA, 2004. Impacts of a Warming Arctic: Arctic Climate Impact Assessment. ACIA Overview report. Cambridge University Press. 140 pp.

Amundsen L., Landrø M. Gas Hydrates - Part I: Burning Ice. *GeoExPro*. Vol. 9, No. 3 – 2012.

Andieva T.A. Tectonic position and main structures of the Laptev Sea. 2008. *Neftegaz. Geol. Teor. Prakt.*, No. 3, 1-28. (In Russian). Available at: http://www.ngtp.ru/rub/4/8_2008.pdf (Accessed 2 March 2020)

Bauch D., Hölemann J., Willmes S., Gröger M., Novikhin A., Nikulina A., Kassens H., Timokhov L. Changes in distribution of brine waters on the Laptev Sea shelf in 2007. *J. Geophys. Res.* 115, C11008 (2010).

Baza znaniy. Laptev sea. [Electronic resource]. Available at: http://proznania.ru/?page_id=2356 (Accessed 18 January 2020) (In Russian).

Bogoyavlensky V. I., Yanchevskaya A. S., Bogoyavlensky I. V., Kishankov A. V. Gas hydrates in the Circum-Arctic Region aquatories. *Arctic: ecology and economy*, 2018, no. 3 (31), pp. 42—55. DOI: 10.25283/2223-4594-2018-3-42-55. (In Russian).

Collett TS, Lewis R, Uchida T. Growing interest in gas hydrates. *Oilfield Review*, Summer 2000:42-57.

Dobrovolskii, A.D. and Zalogin, B.S., *Morya SSSR (Seas of the Soviet Union)*, Moscow: MGU, 1982. (In Russian).

Drachuk A. Kinetika obrazovaniya i dissociacii gazovyh gidratov v vodnyh dispersnyh sredah, stabilizirovannyh dioksidom kremniya. [Kinetics of the formation and dissociation of gas hydrates in aqueous dispersed media stabilized by silicon dioxide]. Dissertation ... of the candidate of physical and mathematical sciences. FGAOU VO «Tjumenskij gosudarstvennyj universitet». 2018. – 118p. (In Russian).

Ermakova L.A., Nivikhin A.E. Some data on hydrology of the near bottom layer of the Kara Sea using the materials of expeditions of R/Vs Barkalav-2007 and Barkalav-2008. 2011 *Probl. Artc. Antarct.*, No. 3, 89-100 (In Russian)

Fiziko - himicheskie svojstva prirodnogo gaza. Metodicheskoe posobie. Sistema nepreryvnogo firmennogo professional'nogo obrazovaniya kadrov gazovoj promyshlennosti OOO Gazprom transgaz Ekaterinburg filial Uchebno-proizvodstvennyj centr Napravlenie: Transport gaza. [Physical and chemical properties of natural gas. Toolkit. The system of continuing corporate professional education for gas industry personnel Gazprom transgaz Yekaterinburg branch Training and production center Direction: Gas transport.]. GAZPROM Open Joint Stock Company. Chelyabinsk. 2008. (In Russian).

Giustiniani M., Tinivella U., Jakobsson M, Rebesco M. Arctic ocean gas hydrate stability in a changing climate. *Journal of Geological Research* 2013

GUFO.ME. Mining encyclopedia. [Electronic resource] Available at:
https://gufo.me/dict/mining_encyclopedia (Accessed 18 January 2020) (In Russian).

Grigoriev MN, Overduin PP, Wetterich S, Sandakov A., Guenther F. Coastal erosion, sediment and organic carbon fluxes in the central sector of the Laptev Sea. Reports on Polar and marine research. Research in the Laptev Sea region. Proceedings of the joint Russian-German workshop. November 8-11, 2010, St. Petersburg, Russia. Edited by Sebastian Wetterich, Paul Pier Overduin, Irina Fedorova with contributions of the participants

Information about Arctic Seas. FSBI “Arctic and Antarctic Research Institute”. Available at: http://www.aari.ru/projects/ECIMOt/Docs/reports/21/html/page_2.html (Accessed 6 March 2020) (In Russian).

JAMES R.H., BOUSQUET P., BUSSMANN I., HAECKEL M., KIPFER R., LEIFER I., NIEMANN H., OSTROVSKY I., PISKOZUB J., REHDER G., TREUDE T., VIELSTÄDTE L. and GREINERT J., 2016 – Effects of Climate Change on Methane Emissions from Seafloor Sediments in the Arctic Ocean: a Review: Methane Emissions from Arctic Sediments. *Limnology and Oceanography*

Kara Sea. Hydrological regime. FSBI “Arctic and Antarctic Research Institute”. Available at:
http://www.aari.ru/resources/a0013_17/kara/Atlas_Kara_Sea_Winter/text/rejim.htm (Accessed 6 March 2020) (In Russian).

Khmelevskoy V.K., Gorbachev Yu.I., Kalinin A.V., Popov M.G., Seliverstov N.I., Shevnin V.A. *Geofizicheskie metody issledovaniy* [Geophysical research methods]. Petropavlovsk-Kamchatskiy, KGPU, 2004. 229 p. (In Russian).

Khutorskoy M.D., Akhmedzyanov V.R., Ermakov A.V. et al. *Geotermiya arkticheskikh morey* [Geothermy of the Arctic seas] 2013. Moscow: «GEOS» Publ. 244 p. (In Russian).

Kiselev A.A., Reshetnikov A.I. Methane in the Russian Arctic: Observation and calculation results. 2013 *Probl. Arktiki i Antarktiki*, No. 2,5-15 (In Russian)

Klitzke, Peter; Luzi-Helbing, Manja; Schicks, Judith M.; Cacace, Mauro; Jacquy, Antoine B.; Sippel, Judith; Scheck-Wenderoth, Magdalena; Faleide, Jan Inge. Gas Hydrate Stability Zone of the Barents Sea and Kara Sea Region / *Energy Procedia*. 97 (2016), 302 – 309.

Kulakov M.Yu., Pogrebov V.B., Timofeyev S.F. et al. Ecosystem of the Barents and Kara Seas coastal segment // *The Global Coastal Ocean. Interdisciplinary Regional Studies and Syntheses* / Edited by A.R. Robinson and K.H. Brink. The Sea: Ideas and Observations on Progress in the Study of the Seas. Vol. 14. Harvard University Press. Cambridge, MA, 2004. P. 1139-1176.

Malakhova V.V. Golubeva E.N., Eliseev A.V., Platov G.A. Estimation of possible climate change impact on methane hydrate in the Arctic Ocean // IOP Conf. Series: Earth Environ. Sci. 2018. V. 211. 012017

Natural Gas Hydrates in Flow Assurance. Carolyn Ann Koh, Amadeu Sum, E. Dendy Sloan 2010

Nauchno-obosnovannye predlozheniya po razrabotke i metodam vnedreniya innovacionnyh tehnologij utilizacii vybrosov, soderzhashhih metan. [Science-based proposals for the development and implementation methods of innovative technologies for the disposal of methane-containing emissions]. CLOSED JOINT STOCK COMPANY "UGLEMETAN SERVICE" Kemerovo 2015 (in Russian).

Portnov A., Mienert J., Serov P. Modeling the evolution of climate sensitive Arctic subsea permafrost in regions of extensive gas expulsion at the West Yamal shelf // J. Geophys. Res.: Biogeosciences. – 2014. – V. 119 (11). - P. 2082-2094.

Reshetnikov A. A., Golovanchikov A. B. Formation of gas hydrates and methods of their extraction//Izvestiya Volgogradskogo gos-go un-ta: mezhvuz. sbornik nauch. st. VolgGTU//Seriya Reologiya, processy i apparaty him. tehnologii. – Volgograd. – 2010. – Iss. 1(61). – P. 5–7. (In Russian)

Romankevich E.A. Carbon cycle in the Arctic seas/ II international scientific conference "Open Arctic". 2015 (In Russian)

Romankevich E.A., Vetrov A.A., Peresypkin V.I. Organic matter of the World Ocean. Russian Geology and Geophysics. 2009. T. 50. № 4. C. 299-307. (In Russian).

Romanovskii, N. N., H. W. Hubberten, A. V. Gavrilov, A. A. Eliseeva, and G. S. Tipenko (2005), Offshore permafrost and gas hydrate stability zone on the shelf of East Siberian Seas, Geo-Marine Letters, 25(2-3), 167-182

Ruppell C. Methane Hydrates and the Future of Natural Gas/ Gas Hydrates Project 2011

Serov P., Portnov A., Mienert J., Semenov P. & Ilatovskaya P. (2015). Methane release from pingolike features across the South Kara Sea shelf, an area of thawing offshore permafrost. Journal of Geophysical Research - Earth Surface, 120(8), 1515-1529.

Serov, P., Vadakkepuliambatta, S., Mienert, J., Patton, H., Portnov, A. D., Silyakova, A., ... Hubbard, A. L. (2017). Postglacial response of Arctic Ocean gas hydrates to climatic amelioration. Proceedings of the National Academy of Sciences of the United States of America, 114(24), 6215-6220

Sloan, E.D. Clathrate hydrates of natural gases / E.D. Sloan, C.A. Koh. - CRC Press. - 2008. - 720 p.

Sloan E., Offshore Hydrate Engineering Handbook, SPE Monograph vol. 21 (1998).

Streletskaya Irina D., Vasiliev Alexander A., Vanstein Boris G. Erosion of Sediment and Organic Carbon from the Kara Sea Coast. *Arctic, Antarctic, and Alpine Research*, Vol. 41, No. 1, 2009, pp. 79–87

Soloviev V.A., Ginsburg G.D., Telepnev E.V., Mikhalyuk Yu.N. Cryogeothermics and Natural Gas Hydrates within the Interior of the Arctic Ocean. Leningrad: PGO «Sevmorgeologiya», 1987, p. 150 (in Russian).

Streletskaya I.D., Vasiliev A.A., and Vanstein B.G. Erosion of sediment and organic carbon from the Kara Sea coast. 2009. *Arctic, Antarctic. And Alpine Research* 41: 79-87.

Vetrov A. A., Lobus N. V., Drozdova A. N., Belyaev N. A., Romankevich E. A. Methane in Water and Bottom Sediments in Three Sections in the Kara and Laptev Seas. March 2018 *Oceanology* 58(2):198-204

Vorobyev A.E., Malyukov V.P. Gas hydrates. The impact of technology on unconventional hydrocarbons. – M. : RUDN, 2009. – p. 289

Whiticar, M.J. (1999) Carbon and Hydrogen Isotope Systematics of Bacterial Formation and Oxidation of Methane. *Chemical Geology*, 161, 291-314

Yakushev, V.S. Natural gas and gas hydrates in cryolithozone. 2009, Moscow, vNiiGas, 192 pp. (in Russian).

Attachments

Attachment 1. Characteristics of GHSZ for 4 gas mixtures in compositions of gas hydrates

Point №	Seafloor depth/ Top of GHSZ, m	Base of GHSZ (100% CH ₄), m	Base of GHSZ (99% CH ₄ / 1% C ₂ H ₆), m	Base of GHSZ (95% CH ₄ / 5% C ₂ H ₆), m	Base of GHSZ (90% CH ₄ / 10% C ₂ H ₆), m	Thickness of GHSZ (100% CH ₄), m	Thickness of GHSZ (99% CH ₄ / 1% C ₂ H ₆), m	Thickness of GHSZ (95% CH ₄ / 5% C ₂ H ₆), m	Thickness of GHSZ (90% CH ₄ / 10% C ₂ H ₆), m
1	255	-	586	705	790	-	331	450	535
2	433	875	900	975	1037	442	467	542	604
3	530	1005	1025	1100	1145	475	495	570	615
4	450	910	940	1010	1070	460	490	560	620
5	620	1160	1175	1230	1285	540	555	610	665
6	550	1060	1080	1140	1200	510	530	590	650
7	250	-	-	650	740	-	-	400	490
8	380	790	810	900	965	410	430	520	585
9	28	-	-	-	-	-	-	-	-
10	375	610	630	700	755	235	255	325	380
11	422	660	680	740	790	238	258	318	368
12	255	-	-	490	560	-	-	235	305
13	381	600	625	695	745	219	244	314	364
14	360	595	615	680	735	235	255	320	375
15	190	-	-	-	480	-	-	-	290
16	500	785	805	855	905	285	305	355	405

Attachment 2. Characteristics of GHSZ for gas hydrates with 100 % of methane during late Pleistocene

Point №	Bottom temperature, C°	Bottom temperature, K	Bottom salinity, ‰	Seafloor depth/ Top of GHSZ, m	Calculated top of GHSZ, m	Base of GHSZ (100% CH ₄), m	Thickness of GHSZ (100% CH ₄), m
1	-1.75	271,4	35	155	262	-	-
2	-1.75	271,4	35	333	262	730	397
3	-1.75	271,4	35	430	262	900	470
4	-1.75	271,4	35	350	262	760	410
5	-1.75	271,4	35	520	262	1050	530
6	-1.75	271,4	35	450	262	920	470
7	-1.75	271,4	35	150	262	-	-
8	-1.75	271,4	35	280	262	630	350
9	-15	263,15	35	0	197	-	-
10	-1.75	271,4	35	275	262	440	165
11	-1.75	271,4	35	322	262	530	208
12	-1.75	271,4	35	155	262	-	-
13	-1.75	271,4	35	281	262	450	169
14	-1.75	271,4	35	260	262	-	-
15	-1.75	271,4	35	90	262	-	-
16	-1.75	271,4	35	400	262	660	260

Attachment 3. Methane fluxes

Point №	Corg content (%)	Corg (g/kg)	CH ₄ (g/kg)	CH ₄ (ppm)	CO ₂ (g/kg)	CO ₂ (ppm)	CH ₄ measured (ppm)
1	2	49,88	13,28	13280	36,52	36520	200
2	2	49,88	13,28	13280	36,52	36520	200
3	2	49,88	13,28	13280	36,52	36520	200
4	2	49,88	13,28	13280	36,52	36520	200
5	2	49,88	13,28	13280	36,52	36520	200
6	2	49,88	13,28	13280	36,52	36520	200
7	1	25,12	6,72	6720	18.48	18480	200
8	1	25,12	6,72	6720	18.48	18480	200
9	0.5	12,56	3,36	3360	9.24	9240	200
10	1	25,12	6,72	6720	18.48	18480	200
11	0,5	12,56	3,36	3360	9.24	9240	200
12	1	25,12	6,72	6720	18.48	18480	200
13	1	25,12	6,72	6720	18.48	18480	200
14	0,5	12,56	3,36	3360	9.24	9240	200
15	2	49,88	13,28	13280	36,52	36520	200
16	1	25,12	6,72	6720	18.48	18480	200